



Annual variability of ice-nucleating particle concentrations at different Arctic locations

Heike Wex¹, Lin Huang², Wendy Zhang², Hayley Hung³, Rita Traversi⁴, Silvia Becagli⁴, Rebecca J. Sheesley⁵, Claire E. Moffett⁵, Tate E. Barrett⁵, Rossana Bossi⁶, Henrik Skov⁶, Anja Hünnerbein¹, Jasmin Lubitz¹, Mareike Löffler^{1,a}, Olivia Linke¹, Markus Hartmann¹, Paul Herenz^{1,b}, and Frank Stratmann¹

¹Experimental Aerosol and Cloud Microphysics, Leibniz Institute for Tropospheric Research (TROPOS), Leipzig, Germany

²Climate Research Division, Atmospheric Science & Technology Directorate, STB, Environment & Climate Change Canada, Toronto, Canada

³Air Quality Processes Research Section, Environment & Climate Change Canada, Toronto, Canada

⁴Department of Chemistry “Ugo Schiff”, University of Florence, Florence, Italy

⁵Department of Environmental Science, Baylor University, Waco, Texas, USA

⁶Department of Environmental Science, iCLIMATE, Aarhus University, Roskilde, Denmark

^anow at: Deutscher Wetterdienst, Zentrum für Agrarmeteorologische Forschung Braunschweig (ZAMF), Braunschweig, Germany

^bnow at: Senate Department for the Environment, Transport and Climate Protection, Berlin, Germany

Correspondence: Heike Wex (wex@tropos.de)

Received: 7 December 2018 – Discussion started: 18 December 2018

Revised: 26 March 2019 – Accepted: 27 March 2019 – Published: 17 April 2019

Abstract. Number concentrations of ice-nucleating particles (N_{INP}) in the Arctic were derived from ground-based filter samples. Examined samples had been collected in Alert (Nunavut, northern Canadian archipelago on Ellesmere Island), Utqiagvik, formerly known as Barrow (Alaska), Ny-Ålesund (Svalbard), and at the Villum Research Station (VRS; northern Greenland). For the former two stations, examined filters span a full yearly cycle. For VRS, 10 weekly samples, mostly from different months of one year, were included. Samples from Ny-Ålesund were collected during the months from March until September of one year. At all four stations, highest concentrations were found in the summer months from roughly June to September. For those stations with sufficient data coverage, an annual cycle can be seen. The spectra of N_{INP} observed at the highest temperatures, i.e., those obtained for summer months, showed the presence of INPs that nucleate ice up to -5°C . Although the nature of these highly ice-active INPs could not be determined in this study, it often has been described in the literature that ice activity observed at such high temperatures originates from the presence of ice-active material of biogenic origin. Spectra observed at the lowest temperatures, i.e., those derived

for winter months, were on the lower end of the respective values from the literature on Arctic INPs or INPs from mid-latitude continental sites, to which a comparison is presented herein. An analysis concerning the origin of INPs that were ice active at high temperatures was carried out using back trajectories and satellite information. Both terrestrial locations in the Arctic and the adjacent sea were found to be possible source areas for highly active INPs.

1 Introduction

The Arctic warms faster than any other region on Earth, a phenomenon known as Arctic amplification (Serreze and Barry, 2011; Cohen et al., 2014; IPCC, 2013). Many different processes, some of which are heavily interconnected, contribute to this (Pithan and Mauritsen, 2014). However, not all of these processes and feedbacks are fully understood, and some might even still be unknown. Clouds in the Arctic are special in that they often form extended, persistent, low-level stratiform cloud layers, which are kept stable for days by different feedback processes (Shupe et al., 2006, 2013;

Morrison et al., 2012). These clouds influence the energy budget and generally warm the surface compared to clear skies (Intrieri et al., 2002). They often contain supercooled liquid water. In the range of temperatures (T) down to -20°C , fractions of supercooled liquid clouds were reported to be above 50 % based on annual mean data for Europe and North America (both including the Arctic) from satellite remote sensing (Choi et al., 2010). For a multiyear analysis of all clouds, based on ground-based remote sensing at two western Arctic locations (Eureka and Utqiagvik), clouds containing only liquid water occurred at least 20 % of the time in all months with a maximum of 56 % in September (Shupe, 2011). Also, during two Arctic aircraft campaigns operating out of Inuvik, each in April and May of two different years, based on in situ measurements, at least 60 % of the clouds observed down to -18°C were characterized as mostly liquid (Costa et al., 2017).

Ice nucleation forms primary ice in clouds, and for T from 0 to roughly -38°C , ice-nucleating particles (INPs) are needed to induce this nucleation process. Not many measurements of number concentrations of INPs (N_{INP}) in the Arctic have been done up to now; however, these particles play an important role in the lifetime and radiative effects of Arctic stratiform clouds. A number of effects of ice in clouds are described in Prenni et al. (2007), including the fact that ice clouds are optically thinner than supercooled liquid water clouds so that the former emit less longwave radiation towards the surface. A modeling study showed that an increase in N_{INP} may cause a faster dissipation of these stratiform clouds (Loewe et al., 2017), which in turn will influence the surface energy budget. But it should also be mentioned that N_{INP} values of $> 1 \text{ L}^{-1}$ were needed to obtain an effect in this modeling study, and such concentrations were observed for midlatitude regions only for T below $\approx -15^{\circ}\text{C}$ (Peters and Wright, 2015; O'Sullivan et al., 2018). Recycling of INPs was assumed to be possible in Arctic clouds, again based on a modeling study (Solomon et al., 2015); i.e., ice crystals falling from a cloud could sublime and re-entrain into clouds from below, which might potentially enhance the effect of changes in N_{INP} . It also has been shown with large-eddy simulations that ice crystal number concentrations significantly influence cloud structure and the evolution of Arctic mixed-phase clouds (Ovchinnikov et al., 2014). Overall, the cloud phase (i.e., supercooled water versus ice) is important for the radiation budget and hence the effect of Arctic stratiform clouds on climate. Kalesse et al. (2016) examined in detail a mixed-phase stratiform Arctic cloud and its phase transitions for roughly 1.5 d. Observed changes in the cloud were related to changes in air mass, but it was also said explicitly that for a better understanding of cloud phase transitions, among other observations, measurements of N_{INP} are also needed. All of this highlights the importance of insight on the abundance of INPs in the Arctic and on their sources and sinks.

In the past, some studies on Arctic INPs were done. However, most studies only included samples collected during short-term deployments. A comparison of results of the present study with some of those from the literature will be made further down in Sect. 4, while the main outcomes of these previous studies are already described in the following. In general, it can still be said that data on Arctic N_{INP} are scarce, which is particularly true for data at high T . Borys (1983, 1989) derived N_{INP} based on ground-based and aircraft measurements, respectively. It was suggested that mid-latitude pollution did not contribute INPs to Arctic aerosol, as N_{INP} values were found to be lowest in winter when Arctic haze, originating from anthropogenic pollution, was present. Bigg (1996) measured INPs during a ship cruise in the Arctic in the months from August to October. It was concluded that INPs were oceanic in origin, while land was only a weak source, and that the upper troposphere was deficient in INPs. Bigg and Leck (2001) derived N_{INP} also during an Arctic ship cruise in July to September and found a decline in N_{INP} during that phase. At least for some of the detected INPs, the most likely sources were assumed to be bacteria and fragments from marine biota emitted via bubble bursting from the open sea. Rogers et al. (2001) detected INPs during aircraft measurements in the Arctic during the month of May. They reported strongly varying concentrations and found some INPs that contained Si that were likely mineral dust particles, while other INPs seemed to consist of low-molecular-weight components. Prenni et al. (2007) also took aircraft measurements of N_{INP} in the vicinity of Arctic clouds during fall, but they reported lower values than those obtained by Rogers et al. (2001) in spring. It was concluded that typical Arctic values for N_{INP} might be overestimated by current parameterizations. Mason et al. (2016) derived N_{INP} for size-segregated aerosol samples collected between the end of March and July in Alert. N_{INP} values derived from these Alert samples were slightly below values reported for other more southerly stations (mostly in Canada) in that study. They also found that at all stations large fractions of INPs were contributed by supermicron particles. These fractions were generally largest at the highest T at which measurements were made, i.e., at -15°C ; for the Alert samples, $> 90\%$ and 70% of all INPs were > 1 and $> 2.5 \mu\text{m}$, respectively. Similarly, Si et al. (2018) found a size-dependent ability of particles nucleating ice for samples collected mostly in coastal areas in southern Canada and one sample collected in Lancaster Sound in the Canadian Arctic, with larger particles being more ice active. They also concluded that sea spray aerosol was not a major contributor to INPs for the samples taken in southern Canada. Based on concentrations of K-feldspar taken from a global model, N_{INP} values measured at -25°C were modeled well, while INPs ice active at -15°C were missing in this model. Also, Creamean et al. (2018a) reported a strong size dependence of the ice activity in samples collected on land in the northern Alaskan Arctic, where again the largest particles in the

supermicron size range were the most efficient INPs. During sampling phases from March until mid-May, when grounds were covered in snow and ice, number concentrations of the supermicron INPs were lower than those in late May by up to 2 orders of magnitude. The increase in N_{INP} was suggested to originate from open leads in the sea ice and from open tundra. Similarly, for a coastal mountain station in northern Norway (at 70° N), based on four filters sampled during July, Conen et al. (2016) observed that air masses were enriched in INPs ice active at -15°C when they had passed over land. An origin of these INPs from decaying leaves was suggested. Irish et al. (2019) derived N_{INP} during a ship cruise in the Canadian Arctic marine boundary layer in summer. They suggest that mineral dust contributed more strongly to the observed INPs than sea spray, with mineral dust particles likely originating in the Arctic (Hudson Bay, eastern Greenland, north-west continental Canada).

Different substances are known to contribute to atmospheric INPs, as outlined in a number of review articles (Szyrmer and Zawadzki, 1997; Hoose and Moehler, 2012; Murray et al., 2012; Kanji et al., 2017). In general, it is known that N_{INP} increases roughly exponentially with decreasing T , although at higher T steep increases may be observed, followed by a weaker increase or even a plateau region down to roughly -20°C (as seen in, e.g., Petters and Wright, 2015; O'Sullivan et al., 2018; Creamean et al., 2018b). Ice nucleation at higher T is typically related to macromolecules from biogenic entities as bacteria, fungal spores, lichen, pollen, and marine biota. These ice-active macromolecules nucleate ice from just below 0°C down to roughly -20°C (Murray et al., 2012; Kanji et al., 2017; O'Sullivan et al., 2018). Biogenic INPs typically occur in low concentrations in the atmosphere, but nevertheless, at remote marine locations such as the Southern Ocean, where N_{INP} is generally low, marine biogenic INPs might make up a large fraction or even the entire INP population (Burrows et al., 2013; McCluskey et al., 2018a). At less remote locations, the majority of atmospheric INPs consist of mineral dust particles originating from deserts or soils. Pure mineral dust particles of atmospherically relevant sizes typically are ice active below -15°C (Murray et al., 2012; Kanji et al., 2017) or even below -20°C (Augustin-Bauditz et al., 2014) and, with the abovementioned exception of remote marine locations, typically occur at much higher concentrations than biogenic INPs (Murray et al., 2012; Petters and Wright, 2015). However, mineral dust particles might also occur together with biogenic ice-active material (Tobo et al., 2014; O'Sullivan et al., 2014; Hill et al., 2016), and such a mixed particle acts like a biogenic INP (Augustin-Bauditz et al., 2016) and should be attributed to the aforementioned group of biogenic INPs.

The existence of particularly high fractions of supercooled water observed in Arctic stratiform clouds, as, e.g., observed in Costa et al. (2017) in the temperature range above -20°C in comparison to more convective clouds in midlatitudes and

the tropics, could be expected to be linked to a lack of biogenic INPs in the Arctic due to sparse biological activity. However, it is known that biogenic INPs are contained in seawater (Schnell, 1977) and the oceanic surface microlayer (SML) (Wilson et al., 2015; Irish et al., 2017) and are emitted to the atmosphere by sea spray production (DeMott et al., 2016). An increase in INP concentrations in the SML (Wilson et al., 2015) and for the biosphere in general (Schnell and Vali, 1976) from equatorial regions towards the poles has been observed. Also present in the Arctic are fungi (Fu et al., 2013), lichen, and bacteria (Santl-Temkiv et al., 2018), which could potentially contribute biogenic INPs.

In the present study, we aimed at increasing the knowledge of Arctic surface concentrations of INPs active in the immersion freezing mode, as described in the following. The immersion freezing mode was examined as it has been described as the most important heterogeneous ice nucleation mode in mixed-phase clouds (Ansmann et al., 2009; Wiacek et al., 2010; de Boer et al., 2011). No specific measurement campaign was organized for the examinations described herein. Instead, use was made of already existing filter samples. Besides for deriving temperature spectra of N_{INP} for 104 filter samples (Sect. 3.1), we also determined possible sources for INPs that are ice active at high T for selected samples. For that, correlations between N_{INP} and some chemical compounds were made (Sect. 3.2.1), and an analysis was done concerning possible regions of origin of INPs that are ice active at high T (Sect. 3.2.2) for a selection of samples. The results will also be discussed in light of literature data (Sect. 4).

2 Measurements

Quartz-fiber filters were sampled regularly at the four Arctic measurement stations of Alert, Ny-Ålesund, Utqiagvik, and Villum Research Station (VRS) during the past years. Figure 1 shows the locations of these four stations, which are all in close proximity to the ocean ($< 3\text{ km}$). A portion of the filters was provided for the analysis presented herein. In the following, some detail will be given on these four different stations, including the filter handling, and on the measurement and evaluation method used to obtain INP number concentrations. We also describe in detail the temperature history of the filters, although it is not yet known with certainty how the temperature during storage will affect INP concentrations. Generally, the filters were kept frozen whenever possible. Transport from the four institutes where the samples had been kept to TROPOS was done in insulated boxes, together with cooling elements. The shipment was organized such that transport was fast (1–3 d) and that upon arrival at TROPOS the temperature in the boxes was still below 0°C . At TROPOS, samples were again stored at -18°C until the measurements were done. These measures during storage and transport are precautions, as for biogenic INPs, storage at

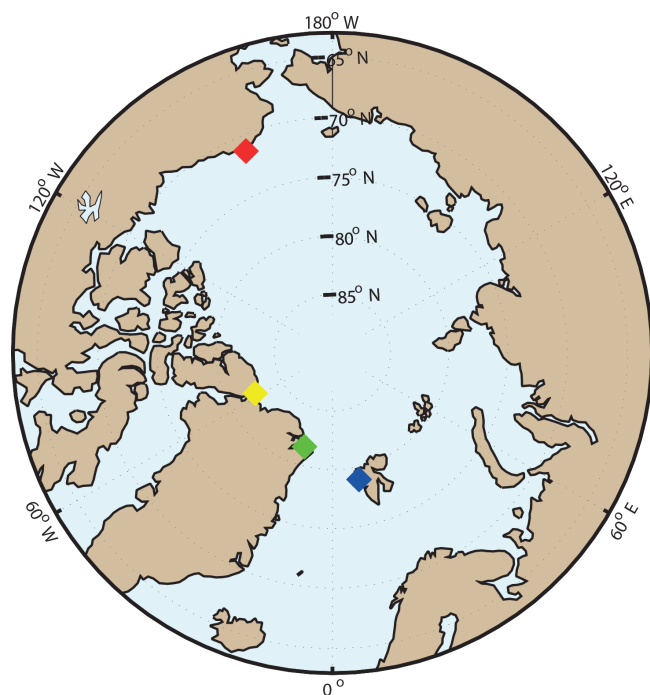


Figure 1. The location of the four stations from which filter samples were included herein: Utqiagvik (red diamond), Alert (yellow diamond), VRS (green diamond), and Ny-Ålesund (blue diamond).

temperatures above 0 °C or even storage under freezing conditions has been found to reduce their ice activity (Wex et al., 2015; Polen et al., 2016, respectively). In this study, unless mentioned otherwise, all samples from all stations (also including field blanks) were treated similarly during all procedures. In the next sections, peculiarities of the separate four stations are described, followed by details of the measurements and their evaluation.

2.1 Alert

A custom-built high-volume aerosol sampler was used at the Dr. Neil Trivett Global Atmosphere Watch Observatory in Alert, Canada (82°30' N, 62°22' W; 210 m above sea level, a.s.l.), to collect 38 samples between April 2015 and April 2016. The sampler is installed at a walk-up deck about 4 m above the ground. The flow rate is approximately 1.4 m³ min⁻¹ at standard temperature and pressure (STP) conditions. Quartz filters (8 × 10 in; Pall Life Sciences, Pallflex filters, USA) were pre-fired at 900 °C overnight and then shipped to Alert while already loaded on cartridges. During transport and storage, the filter-containing cartridges were wrapped with aluminum foil, and they were inside sealed plastic bags. Sampling time for those filters was either 1 week or 2 weeks, the latter being used from August until October (due to operational issues, no filter was sampled in July). A total of nine field blanks (roughly one every month) were collected. These field blanks were treated sim-

ilarly to the other filters, i.e., inserted into the sampler for 2 min, but without an airflow through them. They were also stored similarly to the sampled filters at all times. After sampling, filters were stored (at room temperature ≈ 20 °C) in their sampling cartridges (wrapped in aluminum foil inside sealed plastic bags) at the Alert station and shipped in cardboard boxes (containing five sampling cartridges each) to the Toronto lab at Environment Climate Change Canada where they were stored frozen at < -30 °C. From these filters, a circular piece 47 mm in diameter was shipped to Leipzig for this study.

The total sampling area on the filters was 17.8 cm × 22.8 cm. For the measurements at TROPOS, described in detail in Sect. 2.5 below, circles with 1 mm diameter were punched out from the samples using sterile biopsy punches and immersed in ultrapure water separately. The volume of air sampled per 1 mm piece of filter differed for the different samples and varied from roughly 270 to 540 L.

2.2 Ny-Ålesund

Filter sampling in Ny-Ålesund on Svalbard (at 78°55' N, 11°55' E; 11 m a.s.l.) is done by the University of Florence, Italy. Quartz-fiber filters have been sampled regularly since 2010 using a high-volume sampler with quartz microfiber filters (CHMLAB Group QF1 grade, Barcelona, Spain). The filters were pretreated at 400 °C prior to sampling. The filters had a diameter of 47 mm, one-quarter of which was provided for the present study. Sampling duration was 4 d in 2012, and of these filters, 13 sampled from late March until the beginning of September were examined in the present study, together with two field blanks. The total air volume collected on each filter was roughly 200 m³. Each circular 1 mm filter piece used for the analysis sampled particles from roughly 130 L. Once sampled, filters were stored in a freezer at the Italian base in Ny-Ålesund and then shipped to Italy via cargo. At the home university, they were then stored in a cold room at -20 °C.

2.3 Utqiagvik (formerly known as Barrow)

Filter sampling in Utqiagvik, Alaska (at 71°18' N, 156°46' W; 11 m a.s.l.), is done by Baylor University, US, as described in Barrett and Sheesley (2017). For the present study, quartz-fiber filters were used that had been sampled regularly in an annual campaign from June 2012 to June 2013 using a high-volume sampler (Tisch Environmental, Cleves, OH, USA). Filters were stored frozen prior to and immediately following all sampling. Two rectangular filter pieces (with a lateral length of 1.5 cm) from each of 41 different filters and two field blanks were provided for the present study. The sampled area of each filter was 399 cm². Sampling on each filter was done for 4 up to 13 d (7 d on average), collecting particles from a total air volume of

roughly 14 000 to 51 000 m³. This yields an air volume of roughly 270 to 1000 L collected on each circular 1 mm filter piece used for the analysis. Prior to sampling, filters were pretreated at 500 °C. After sampling, the filters were stored in a freezer on-site and transported to the home university in coolers with cooling elements, where they were then stored at −18 °C.

2.4 Villum Research Station

Villum Research Station (VRS) at Station Nord in northern Greenland (at 81°36' N, 16°40' W; 24 m a.s.l.) is operated by Aarhus University, Denmark (in cooperation with the Danish Defense, the Arctic Command). Quartz-fiber filters have been sampled regularly since 2008 using a high-volume sampler (DIGITEL Hegnau, Switzerland) and employing weekly sampling (Bossi et al., 2016). The filters had an exposed area of 154 cm² and sampled a total air volume of roughly 5000 m³. From filters sampled in 2015, a 2 cm diameter piece was cut from each of the filters and provided for this study. Due to the large interest in shares of the filters, only samples from 11 different filters, all from different months in 2015 and 1 from December 2013, could be used herein. As for all samples used in this study, from the 2 cm pieces punches of 1 mm in diameter were cut at TROPOS directly prior to the measurements. The resulting small pieces were then used for INP analysis. The area of these 1 mm pieces corresponds to a sample volume of 255 L of air. Prior to sampling in the field, filters were pretreated at 450 °C. Storage of the filters at VRS was done in freezers. Filters are transported from Greenland to Denmark around three times per year by the Danish Royal Air Force and then shipped to Roskilde, where they were then stored at −18 °C.

2.5 Freezing device INDA, the Ice Nucleation Droplet Array

For freezing experiments examining immersion freezing, a device comparable to one introduced in Conen et al. (2012) was used, but deploying PCR trays (Hill et al., 2016) instead of separate tubes. The same device had been used in Chen et al. (2018). From each filter piece that had been shipped to TROPOS, circles with a diameter of 1 mm were punched out directly before measurements were done, and each of the 96 wells of a PCR tray was filled with such a filter piece together with 50 µL of ultrapure water (background measurements of ultrapure water are given in the Supplement). After sealing the PCR tray with a transparent foil, it was immersed into a bath thermostat such that the water table in the wells was below the surface of the liquid in the thermostat. The bath of the thermostat was then cooled with a cooling rate of 1 K min^{−1}, and the freezing process was monitored by a camera, taking a picture every 6 s. An LED light source installed below the PCR tray ensured that wells in which the water was still liquid could be easily distinguished from frozen ones.

Frozen fractions (f_{ice}) were then determined as the number of frozen tubes divided by the total number of tubes. Typically, fresh water to be used in the experiments was taken once a day and stored in a glass bottle. Whenever fresh water was taken, an experiment was run with this water in the tubes only to ensure that the water was satisfyingly clean. Similarly, experiments were run with field blank filters that had the same history as the samples but without sampling (see the Supplement), and signals from the field blanks were well below those of the sampled filters. A subtraction of the signals of the field blank from those of the measurements was not done. This is justified in a detailed discussion in the Supplement. The interpretation of the results from the filters presented in this study is the same for both uncorrected and background-corrected samples.

2.6 Deriving N_{INP}

Equation (1) was used to derive N_{INP} from the measured f_{ice} (Vali, 1971; Conen et al., 2012). This equation accounts for the possibility of the presence of multiple INPs in one vial by assuming that the INPs are Poisson distributed. Additionally it normalizes the values resulting from the measurement with the air volume sampled on each 1 mm filter piece. This yields concentrations of ice-nucleating particles per volume of sampled air.

$$N_{\text{INP}} = -(\ln(1 - f_{\text{ice}})) / (F \cdot A_p / A_f) \quad (1)$$

F is the total volume of air drawn through the filter, and A_p and A_f are the surface area of a single 1 mm filter piece and the whole sampled area of the filter, respectively.

The temperature and concentration regions for which data were obtained for the different samples depend on a number of factors. The measured value f_{ice} is a fraction ranging from 0 to 1. Therefore, N_{INP} , as derived using Eq. (1), can only take on a limited range of values. This range is based on the negative natural logarithm of 0.01 and 0.99 (4.6 to 0.01). The absolute values of N_{INP} then also depend on the volume of air sampled onto each 1 mm filter piece, i.e., on the volume of air drawn through the filter during the sampling period and on the relation of the surface area of one filter piece to the total sampled surface area. The volume collected per 1 mm filter piece was within a factor of 4.5 for all filters (120 to 540 L). Altogether, the range of N_{INP} that can be obtained herein is roughly from 2×10^{-5} to 0.04 L^{−1}. From this limitation, it also follows that the range of T for which N_{INP} could be obtained is limited, as it is tied to the concentrations that can be measured. Times with more ice-active INPs show up as N_{INP} at higher T . The highest T at which ice activity was observed was close to −5 °C, as will be shown in the next section.

It should also be noted that samples that had less than 60 L of air volume collected on each 1 mm filter piece were also examined, but f_{ice} was close to the background and therefore these samples were not considered in this study. Results

from background measurements are given in the Supplement. Measurement uncertainty as shown in this work was derived based on Harrison et al. (2016), i.e., following the assumption that the INPs are Poisson distributed between the different examined droplets. The first few droplets that freeze in each experiment therefore show the highest uncertainties.

2.7 Using back trajectories and satellite maps

A more in-depth analysis concerning possible INP source regions was done for a selection of filter samples from each measurement station. For that, 5 d back trajectories were calculated with HYSPLIT (Stein et al., 2015) to determine the origin of sampled air masses. These calculations were based on GDAS (Global Data Assimilation System) meteorological data using an hourly time resolution. A new trajectory was started every 6 h during the whole time for which sampling was done on the respective filter. Back trajectories were initiated at an altitude of 100 m above the sampling locations, as this altitude still has a high likelihood of being connected to the ground and as lower elevations are more prone to uncertainties. In the Supplement, these back trajectories are shown separately for the selected examined filter samples.

Using these back trajectories, we examined over which ground the air masses collected on the filters had passed in the 5 d prior to arrival at the measurement station. The aim was to see contributions from open land or open water for the different selected filter samples. Therefore, a distinction was made between snow, open land, sea ice, and open water. To do so, maps from the Interactive Multisensor Snow and Ice Mapping System (IMS) (Helfrich et al., 2007; National-Ice-Center, 2008, 2008) were used. IMS maps are a composite product produced by NOAA/NEDIS (National Oceanic and Atmospheric Administration's National Environmental Satellite Data and Information Service) combining information on both sea ice and snow cover. Information from 15 different sources of input is included in the production of these maps (Helfrich et al., 2007). These maps have been provided for 20 years. We used the daily Northern Hemisphere maps with a resolution of 4 km (National-Ice-Center, 2008, 2008). For each time step we applied nearest-neighbor interpolation in space and time to find the corresponding satellite coordinate along the back trajectory. With that, for each back trajectory, we determined the conditions on the ground during the passage of the air mass, i.e., if the ground was covered by snow or ice or if open water or open land was present. The resulting information is shown exemplarily in Fig. 4 for the filter samples collected in Alert starting 10 June 2015. Using these maps, we counted how often air masses that were collected on one filter were above open land or open water while the air mass was below 100 m. (As will be discussed in detail in Sect. 3.2.2, for Utqiaġvik, results reported here always refer to an upper altitude of 500 m and 10 d back trajectories.) An altitude restriction was used as we were trying to geographically locate INP sources on the surface. Additionally,

the back trajectories were only considered back in time until an integral amount of 2 mm of precipitation (taken from the information included in the back trajectories) was reached. This was done as precipitation formation occurs via the ice phase so that precipitation is assumed to lead to a washout of INPs.

3 Results

In the following, N_{INP} derived from filter samples will shortly be introduced. A correlation with some available chemical composition data is made. Finally, an analysis of air mass origins is introduced to analyze possible source regions for INPs that are ice active at high T . A comparison to literature data and further discussion of the results are then presented in Sects. 4 and 5, respectively.

3.1 Arctic atmospheric INP concentrations

Quartz-fiber filters from the four different Arctic stations shown in Fig. 1 were analyzed to derive N_{INP} . Figure 2 shows N_{INP} for all different samples separately for the four sampling locations. Due to the comparably large number of filters analyzed for Alert and Utqiaġvik, separate curves cannot be seen easily in Fig. 2. Therefore, Fig. 3 shows time series of N_{INP} for T at -7 , -10 , -13 , and -9.5 °C for Alert, Utqiaġvik, Ny-Ålesund, and VRS, respectively. T was chosen such that N_{INP} could be obtained for the largest possible number of all curves (data for the three samples with the lowest N_{INP} are missing for Alert (29 April and 27 May 2015 and 4 April 2016), as is the one with the highest N_{INP} for Utqiaġvik (3 May 2013), indicated by arrows in Fig. 3). The yellow background shows for which samples an more in-depth analysis is presented in Sect. 3.2.2. Error bars in Fig. 3 show the 95 % confidence interval.

It is worth noting that once a sample has a comparably high concentration at one T this is generally observed at all T at which measurements are available and vice versa; i.e., the curves do not intersect much (see Fig. 2). Therefore, the curves shown in Fig. 3 can be used to discuss observed trends for INPs that are ice active at high T . It should also be noted that for Ny-Ålesund, data only exist for March until September and that for VRS there is mostly only one data point per month, if any (no data exist for February, March, and May).

In Figs. 2 and 3 it can be seen that in general N_{INP} obtained for the summer months is higher than for the winter months. A decrease in N_{INP} is observed starting in fall (October or November). For months with the lowest observed ice activity, which are generally winter and early spring months, values for N_{INP} were measured down to below -20 °C. From June until September mostly INPs that were ice active between -5 and -15 °C were detected (see Fig. 2), and for Utqiaġvik and VRS such highly ice-active INPs were observed as early as April. These highly ice-active INPs will be the focus of the

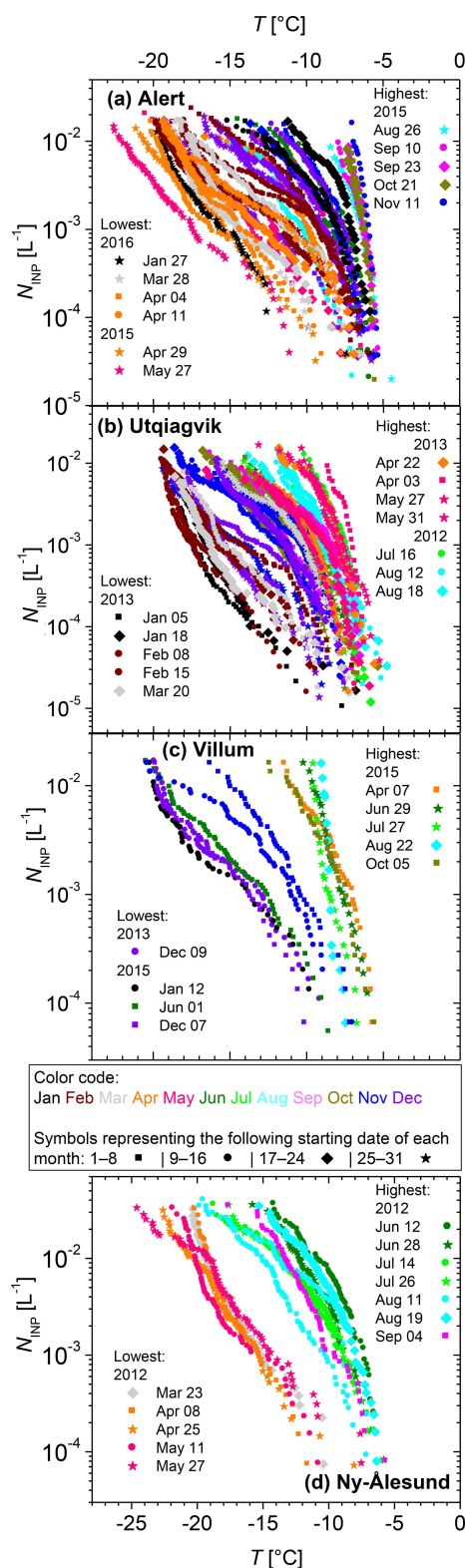


Figure 2. N_{INP} for all samples. Symbol color distinguishes between data obtained for the different months, while symbol type indicates the day of the month when sampling started. Curves with particularly high and low N_{INP} are explicitly listed in the legend. (The T axis is the same for panels a–c and different for panel d; see values for T given on the top and bottom of the figure, respectively.)

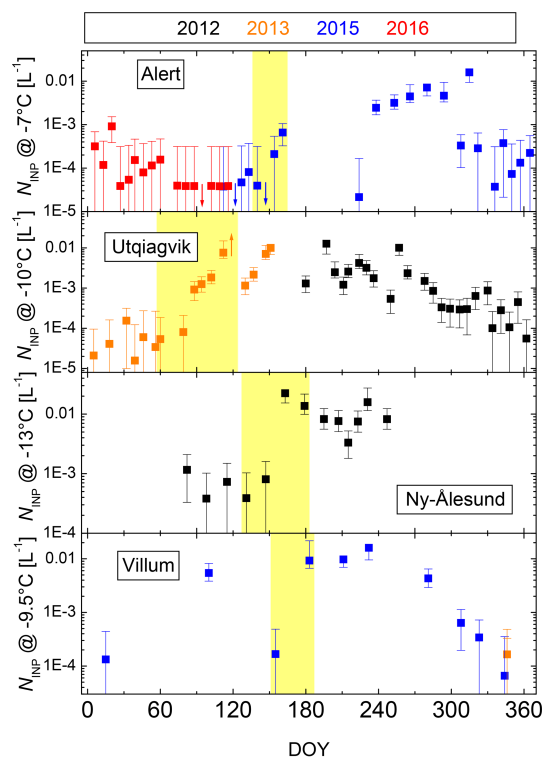


Figure 3. Time series of N_{INP} at T of $-7, -10, -13,$ and -9.5°C for Alert, Utqiagvik, Ny-Ålesund, and VRS, respectively. Small arrows in the panels indicate times when values were either below (for Alert) or above (for Utqiagvik) the detection limit. The yellow background shows for which samples a more in-depth analysis is presented in Sect. 3.2.2. Error bars show the 95 % confidence interval.

next two sections (Sect. 3.2.1 and 3.2.2). Similarly highly ice-active INPs have been suggested to be biogenic in origin based on tests such as heat treatment (Hill et al., 2016; O’Sullivan et al., 2018), which due to the limited available amount of filter material could not be done in the present study.

3.2 Sources of INPs

3.2.1 Correlation to chemical composition

Typical N_{INP} values measured in the atmosphere are several orders of magnitude below total particle number concentrations, and therefore mass concentrations of INPs are so small that a correlation between bulk chemical composition and N_{INP} might not be expected, particularly not for the very rare INPs that are ice active at high T . This is in line with recent findings for a long-term study of INPs at Cape Verde by Welti et al. (2018). There, no correlation between N_{INP} and bulk chemical composition was found for T down to -16°C for a number of different compounds, which included Ca^{2+} , Na^{+} , and elemental carbon as tracers of continental, marine, and combustion sources, respectively. At a lower T of -25°C ,

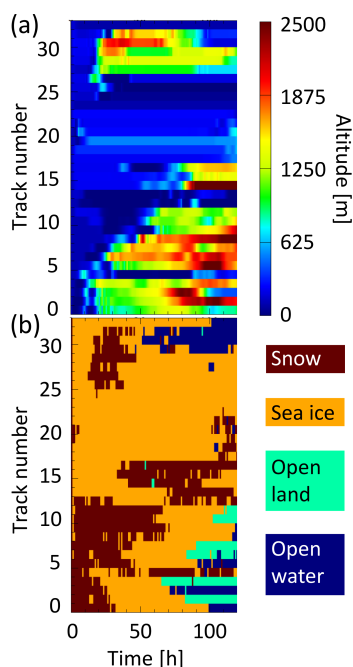


Figure 4. Exemplary results from the analysis of the IMS maps for the filter collected in Alert starting 10 June 2015. In both panels, each row (indicated as track number) represents one trajectory going back in time for 5 d, starting from 0 (when sampling took place), and displaying 120 separate time steps. The colors indicate the altitude of the air mass for the different time steps in panel (a) and the respective nature of the ground at the location of the air mass in panel (b).

Si et al. (2019) recently reported that mineral dust tracers correlated with INPs, which suggests that mineral dust was a major contributor to the INP population at that T . Si et al. (2018) found that for three coastal sites in Canada a model based on K-feldspar as the only INP calculated N_{INP} that fit measurements well at -25°C , while at -15°C measurements were underpredicted, suggesting a missing source of INPs that are active at higher T . In the following we examine whether there is a correlation between the INPs detected in the present study that are ice active at high T and chemical composition.

The examined filters pieces were not particularly sampled for this study and were entirely needed for the above-described INP analysis. No dedicated chemical analysis could be done additionally. But as other parts of most of the filters were also used in other studies, some information on chemical composition was available. This was used to derive the correlations with N_{INP} shown in Fig. 3, i.e., with those INPs that are ice active at high T . Table 1 shows values for R , R^2 , and p for linear correlations between N_{INP} and different bulk chemical properties.

In general, no correlations were found. The only case with a positive value for R (0.59) and a low value for p (0.01) was found for POC+CC (pyrolyzed organic carbon and car-

Table 1. R , R^2 , and p values for linear correlations between N_{INP} (as shown in Fig. 2) and different bulk chemical properties.

Location	Species	R	R^2	p	
Utqiagvik	EC	-0.36	0.13	0.02	
	OC	-0.04	< 0.01	0.82	
	fluoride	0.14	0.02	0.41	
	chloride	0.13	0.02	0.43	
	nitrite	0.22	0.05	0.19	
	bromide	-0.01	< 0.01	0.98	
	sulfate	-0.12	0.01	0.47	
	nitrate	0.03	< 0.01	0.86	
	Ny-Ålesund	PM10	-0.36	0.13	0.22
		OC	-0.39	0.15	0.18
ammonium		-0.44	0.20	0.13	
K		-0.57	0.32	0.04	
Mg		-0.36	0.13	0.22	
nitrite		0.15	0.02	0.62	
nitrate		-0.16	0.03	0.59	
sulphate		-0.60	0.36	0.03	
Na		-0.30	0.09	0.32	
Ca		-0.50	0.25	0.08	
Cl	-0.13	0.02	0.68		
MSA	0.18	0.03	0.55		
Alert	POC+CC	0.59	0.35	0.01	
	OC	-0.12	0.01	0.62	
	EC	0.05	< 0.01	0.84	

bonate carbon) in Alert. Both POC and CC contain carbon that pyrolyzes at 870°C in a pure He stream (Huang et al., 2006). CC might indicate the presence of soil dust (Huang et al., 2006). POC includes some charred carbon formed at 550°C , which is the lower temperature step of the applied analysis (EnCan-total-900 method; Huang et al., 2006; Chan et al., 2010), and highly oxidized organic compounds and/or high-molecular-weight refractory carbon. Based on previous studies, the POC mass is proportional to the oxygen mass in organic aerosols (Chan et al., 2010), releasing as carbon monoxide at 870°C . POC was observed to form from sucrose and glucose (Huang et al., 2006) and therefore might be indicative of biogenic material. This points towards a direction in which more detailed studies should be undertaken in the future. In Sect. 5, we will discuss a range of possible sources for the observed INPs.

3.2.2 Determination of possible source regions

Results from the more in-depth analysis concerning possible INP source regions, based on back trajectories and satellite maps as described in Sect. 2.7, are presented in the following. For this analysis, samples were chosen that had been collected in spring, directly before and after the transition from typical winter to typical summer conditions (see yellow background in Fig. 3). A total of 17 separate filter samples were included: 2 for VRS, 4 each for Alert and Ny-Ålesund,

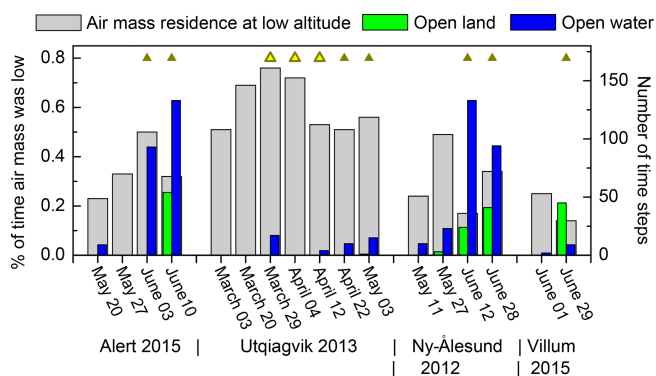


Figure 5. The number of time steps when air masses were at low altitudes and over open land or open water are shown in green and blue, respectively, for different filter samples. The analysis shown was done for altitudes up to 100 m for Alert, Ny-Ålesund, and VRS and up to 500 m for Utqiagvik. Gray bars in the background indicate the percentage of time the air masses collected on each filter were below that altitude. Triangles indicate samples for which highly ice-active INPs were detected, i.e., for which INP spectra were measured at high T (single-colored triangles) and at medium T (triangles with yellow interior). The respective INP spectra are shown in Fig. 6.

and 7 for Utqiagvik. The aim was to see if contributions from open land or open water were potentially more pronounced during times when INPs active at high T were observed.

Figure 5 shows the number of time steps when air masses were over open land or open water for the separate filter samples. Additionally, gray bars in the background indicate the percentage of time the air masses collected on one filter were below 100 m for Alert, VRS, and Ny-Ålesund. It can already be seen that the presence of highly ice-active INPs on a filter is related to air masses that fulfill the above criteria, i.e., that traveled over open land or open water at a low altitude. It also can be seen that this was not found for Utqiagvik. Initially, no open land and hardly any open water had been found for this site when 5 d back trajectories were used, together with an altitude restriction of 100 m, which means that air masses did not travel over open land or open water at altitudes below 100 m. To check if the length of the back trajectory or the chosen maximum altitude influenced our results for Utqiagvik, an analysis was also done using 10 d back trajectories and 500 m as the altitude limit, which is presented in Fig. 5. This extension only resulted in larger percentages of time for which the air masses were below this altitude limit. However, there were still not a large number of time steps found for which air masses traveled over open land or open water for Utqiagvik. We will get back to this again below.

Figure 6 shows the spectra of N_{INP} (called INP spectra for simplicity from now on) for the samples included in this analysis (right side) and the locations where the respective air masses traveled over open land or open water at altitudes below 100 m (or 500 m for Utqiagvik) (left side). Three differ-

ent types of INP spectra can be distinguished: first, there are those for which we observed the start of ice activation only at around -10°C and which went down to well below -15°C . For these, INP spectra and locations are depicted in magenta or orange. Second, there are INP spectra for which we observed ice nucleation from roughly -5 to above -15°C . For these, INP spectra and locations are depicted in greenish colors. The third category was used only for Utqiagvik for INP spectra with medium ice activity depicted in blueish. Error bars shown in Fig. 6 show the 95 % confidence interval.

For Alert, VRS, and Ny-Ålesund, the absence or scarcity of orange and magenta marks on the maps in Fig. 6 (maps on the left in a, b, and c) shows that almost no open land or open water contributed to air masses sampled on the respective filters. This is in accordance with the corresponding INP spectra, which showed comparably low ice activity. The magenta locations close to Svalbard for the Alert sample correspond to the sample from 20 May 2015, for which somewhat more ice-active INPs were found than for the subsequent sample from 27 May 2015. For this latter sample, no contributions from open land or open water were observed, and it is, in fact, the sample with the lowest ice activity observed in this study (see Fig. 2). Locations depicted in greenish colors potentially contributed INPs that are ice active at high T . They can be found on open land as well as on open water. In connection to filters sampled at Alert or at VRS they show up in north Greenland, on Ellesmere Island (on which Alert is located), in Baffin Bay, and along the southern part of the west coast of Greenland. Concerning filters sampled at Ny-Ålesund, greenish marks show up on Svalbard and the adjacent sea.

The above analysis shows that coastal regions may be particularly important as a source for highly ice-active INPs, including open waters close to coasts. Indeed, highly ice-active biogenic INPs were found in Arctic surface waters before (e.g., Wilson et al., 2015; Irish et al., 2017). For the highly ice-active samples collected on Ny-Ålesund on 12 and 28 June 2012, the surroundings of the measurement station were completely snow free during the times when these samples were collected, whereas for all other cases there was at least partial or total snow cover around the stations. In other words, local terrestrial sources close to the measurement station may also contribute as sources for highly ice-active INPs, as already discussed in Creamean et al. (2018a). Also, Irish et al. (2019) describe Arctic landmasses to be the source for observed Arctic INPs (ice active at -15 , -20 , and -25°C), and these INPs were suggested to be mineral dust. On Svalbard, Tobo et al. (2019) found higher atmospheric N_{INP} in July than in March, and they additionally described glacial outwash sediments in Svalbard to be highly ice active. This ice activity was assumed to be connected to small amounts of organic (likely biogenic) material. Based on these findings, Tobo et al. (2019) suggest the higher N_{INP} in summer to be connected to organic (biogenic) components in glacially sourced dust. Some coastal regions in the Arctic,

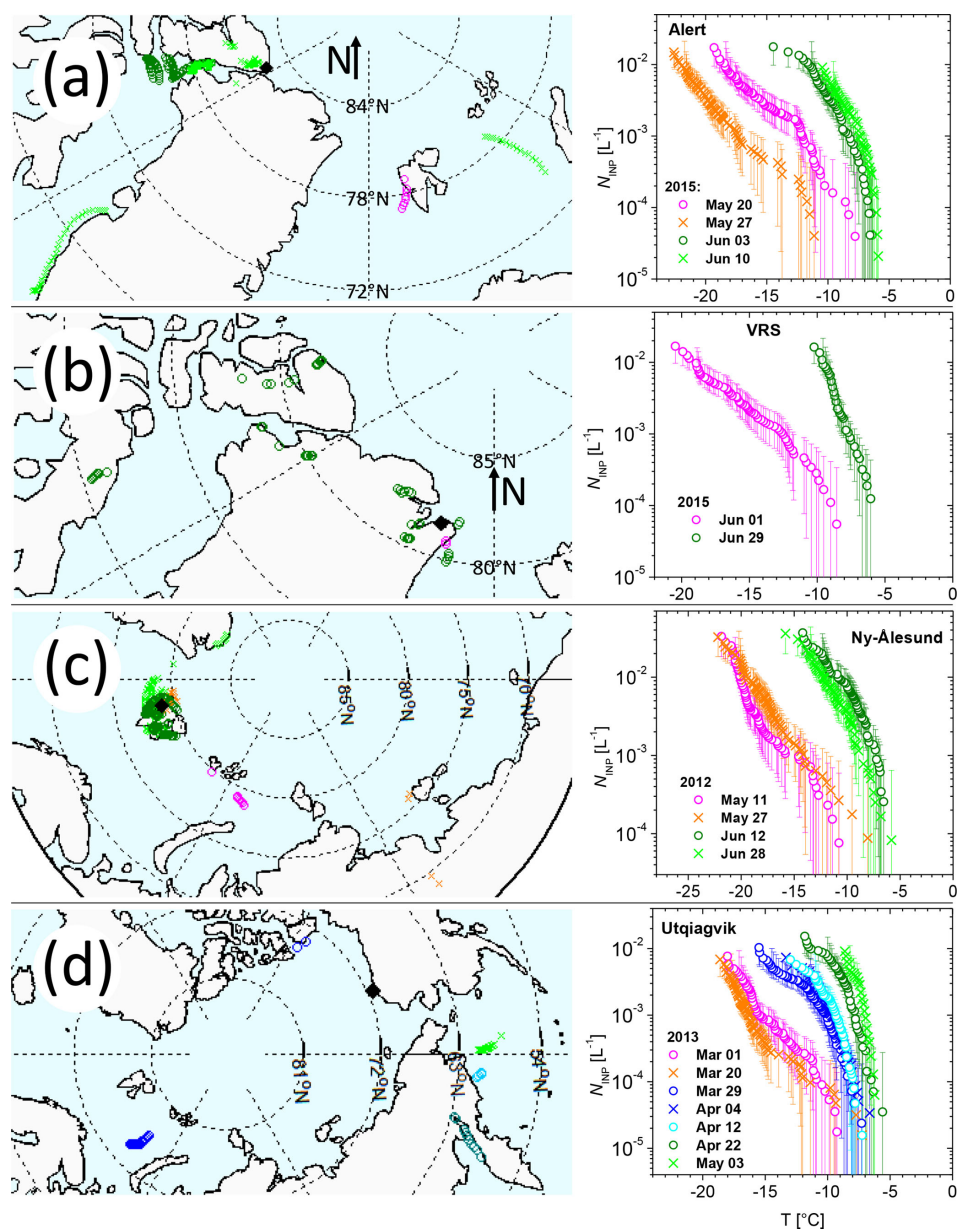


Figure 6. Panels (a), (b), (c), and (d) each show a map on the left side in which locations are indicated where air masses collected on different filters crossed over open land or open water while being at a low altitude (below 100 m for Alert, Ny-Ålesund, and VRS; below 500 m for Utqiagvik). Black diamonds indicate the location of the measurement site. (Please note: the maps in c and d are rotated by 90° compared to the those in a and b.) The right side shows the INP spectra for the corresponding filters.

e.g., the west coast of Greenland together with the region around Baffin Bay and the Canadian Arctic Archipelago as well as the area around the Bering Strait and also Svalbard, are known for their abundance of seabird colonies (Croft et al., 2016). These regions partially coincide with regions highlighted as possible INP sources in Fig. 6. These regions are known to emit ammonia, which plays a role in new particle formation in the Arctic (Croft et al., 2016). But clearly, newly formed particles are not expected to contribute to atmospheric INPs at the temperatures examined in this study,

and INPs are likely also emitted from regions with high biological activity. In Sect. 5 we will discuss possible INP sources in more detail.

For Utqiagvik, data from seven filters were included in the analysis. Two of them showed INP spectra at comparably low T , three at medium T , and two at high T . For all types of INP spectra, no contribution from open land was observed with the back-trajectory analysis. Only minor contributions from open water were found for the latter two types, although the analysis was extended to include 10 d back trajectories,

and the maximum altitude up to which air masses were considered was relaxed to 500 m. Air masses did travel below 100 m, and even more often below 500 m (see Fig. 5 and the back trajectories for Utqiagvik and their heights profiles in the Supplement). However, the transition to filters on which INPs active at comparably high T was already found to happen earlier at Utqiagvik than at the other three measurement locations towards the end of March. IMS maps almost exclusively identified the ground as sea ice and snow in the regions that were crossed by the air masses, even until the beginning of May 2013. And in general, air masses spent more time over sea ice than over snow (see back trajectories in the Supplement). There has to be a source for highly ice-active INPs that was not revealed in the analysis done here. Polynyas and open leads may contribute to explaining this inconsistency. The resolution of the IMS maps used may be too coarse so that open water related to polynyas and open leads could have gone unnoticed.

While the analysis introduced here shows regions that may have potentially contributed highly ice-active INPs to the sampled air masses, it does not make any statement about other regions. Other regions could potentially be sources, too, but might have only been crossed by air masses at high altitudes or may not have been crossed at all.

4 Comparison with literature

Figure 7 shows the ranges of N_{INP} observed for the four stations as shaded areas. Data from the different stations cover a rather similar range. As explained above (Sect. 2.6), N_{INP} could only be measured up to some 10^{-2} L^{-1} , depending on the volume of air sampled onto one 1 mm filter piece. Hence, the upper concentration limit of our data is determined by the measurement method. The gray background shows literature data of N_{INP} determined from precipitation samples collected mostly in North America and Europe (Petters and Wright, 2015). In that data set, samples showing the highest N_{INP} at $T > -20^\circ\text{C}$ originate from rain and hail samples collected in North Carolina (US) and Alberta, Montreal (CA). Some of the INP spectra we detected at the highest T , observed particularly in Alert and Utqiagvik, show values for N_{INP} that are similar or only about 1 order of magnitude below data reported in Petters and Wright (2015). At the lowest temperatures at which we detected INP spectra, N_{INP} values are lower than data from Petters and Wright (2015), i.e., the lowest Arctic N_{INP} , as those we observed in the winter months might be below the lowest values observed on continents in midlatitudes. It is worth adding that still lower concentrations were observed in marine remote locations in the Southern Ocean (McCluskey et al., 2018a) and for clean marine air in the northeast Atlantic (McCluskey et al., 2018b).

Figure 7 shows additional data on Arctic N_{INP} from the literature that were already discussed in the Introduction (Borys, 1983, 1989; Bigg, 1996; Bigg and Leck, 2001; Rogers

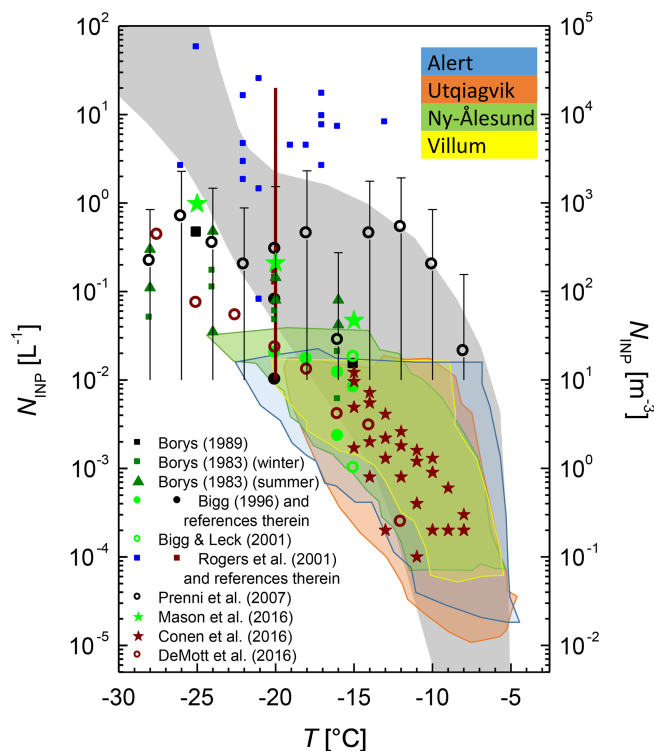


Figure 7. Comparison of N_{INP} determined in this study for the Arctic with literature data by Petters and Wright (2015) (gray background), Borys (1983, 1989), Bigg (1996), Bigg and Leck (2001), Rogers et al. (2001), Prenni et al. (2007), Mason et al. (2016), Conen et al. (2016), and DeMott et al. (2016). Green and brown symbols represent data from surface-based measurements; black and blue represent airborne measurements. For Rogers et al. (2001), brown indicates data they cited from the literature, with the vertical bar indicating the extent of the reported values.

et al., 2001; Prenni et al., 2007; Mason et al., 2016; Conen et al., 2016; DeMott et al., 2016). Not every single data point from these papers is shown, as Fig. 7 aims to give an overview of the range of data that exists. Data on Arctic N_{INP} in general are still scarce, which is particularly true for data at high T . Also, data scatter over a wide range. The highest values of N_{INP} shown in Fig. 7 originate from one set of aircraft measurements made in May (Rogers et al., 2001), while a second set of aircraft measurements, taken in September and October onboard an aircraft flying out of Alaska, agrees with our data at the highest T (Prenni et al., 2007). For the data taken from Prenni et al. (2007), the reported measurement uncertainty is shown, which is representative for typical uncertainties for the type of instrumentation used in Rogers et al. (2001) and Prenni et al. (2007). Error bars indicate 1 standard deviation at the higher end. The lower end is indicative of the detection limit, and for a substantial fraction of measurements no INPs were detected in Prenni et al. (2007).

Going back to Fig. 7, literature data from ground-based measurements that are in the same range of N_{INP} in which

we measured are also within the same T range. But besides the data from Conen et al. (2016), these data are at the lower end of T that we observed. This also holds for the data from DeMott et al. (2016), which were obtained during summer ship cruises in Baffin Bay and in the central Bering Sea.

Data shown for Borys (1983) were taken in Ny-Ålesund and Utqiagvik. A slight tendency towards higher N_{INP} in summer months, compared to winter months, can be seen. Similarly, as said in the Introduction, Bigg and Leck (2001) found a decreasing trend for N_{INP} at -15°C from July to September. The observed decrease was roughly 1 order of magnitude; however, the scatter from sample to sample was almost as large as that trend. Nevertheless, these data sets are early indications of the annual trend that has very clearly been found in the present study.

Concerning possible sources for INPs, Bigg (1996) assumed that mainly oceanic sources contributed to the observed INPs, with only a weak contribution from land. Bigg and Leck (2001) discussed a marine origin of at least some of the INPs they analyzed. These latter two studies were ship based. The land-based study by Conen et al. (2016) showed INPs that were ice active at higher T than those observed in Bigg (1996) and Bigg and Leck (2001). Conen et al. (2016) traced these INPs back to terrestrial contributions, possibly decaying leaves. During aircraft measurements, Rogers et al. (2001) identified some INPs as mineral dust particles and others as containing low-molecular-weight components. These latter might have been connected to biogenic INPs.

These different studies report very diverse N_{INP} . In these studies, different instrumentation was used and sometimes different ice nucleation mechanisms were probed. Also, instrumental limitations typically determine the ranges of T and N_{INP} that can be probed. All of this might add to the diversity in the data. But, as can be seen in Fig. 3, a difference of up to 2 orders of magnitude in N_{INP} was measured between winter and summer for a single temperature in our data set. Therefore, the diversity in N_{INP} reported in previous studies will also originate from different times of the year when these studies were conducted.

All of our samples were collected on land, and regions that showed up as possible sources for highly ice-active INPs in Fig. 6 were on or close to land. While, as said above (Sect. 3.2.2), other regions cannot be excluded as sources, it will be interesting to see in the future if N_{INP} values detected further away from terrestrial sources will consistently be lower than those obtained on land.

Concerning an influence of INPs emitted from the ground at higher altitudes, Herenz et al. (2018) recently compared aerosol particle number size distributions (PNSDs) measured on the ground and during overflights at different heights in May 2014 in Tuktoyaktuk (Northwest Territories of Canada on the Arctic Ocean). PNSDs measured on the ground and at heights up to 1200 m were generally similar, while PNSDs obtained at higher altitudes were clearly different. Therefore, atmospheric aerosol, including INPs, can be similar at

heights up to levels at which cloud formation is observed. Hence, INPs detected by ground-based measurements may well be able to influence ice formation in clouds, at least during times when the cloud layers are coupled to the surface.

Compared to previous literature data introduced in this study, the new long-term data presented here extend the range of Arctic N_{INP} towards higher T . They also clearly show that Arctic INP concentrations vary throughout the year, with a regular presence of INPs that are ice active at T well above -10°C throughout the summer months at all four terrestrial measurement stations.

5 Discussion

The annual cycle observed for N_{INP} in this study is not in tune with what is known for particle number concentrations and size distributions occurring across the Arctic (Tunved et al., 2013; Nguyen et al., 2016; Freud et al., 2017). This is not too surprising: recent studies, including Arctic locations, found that a large fraction of INPs are supermicron in size (Mason et al., 2016; Si et al., 2018; Creamean et al., 2018a), while the majority of particles are in the submicron size range.

Concerning the annual Arctic aerosol cycle, there is a maximum in particle number concentrations in early spring, before precipitation sets in, caused by accumulating anthropogenic pollution known as Arctic haze (Shaw, 1995). N_{INP} values are low during that time of the year, which might indicate that anthropogenic pollution does not contribute to atmospheric INPs, at least in the T range examined in this study. This is in line with the observation that Arctic haze particles are not efficient INPs (Borys, 1989) and also with a recent study showing that anthropogenic pollution did not contribute to INPs in very polluted air in Beijing (Chen et al., 2018). It is also in agreement with observations by Hartmann et al. (2019) based on ice cores from Svalbard and Greenland, who found that N_{INP} in the Arctic did not increase over the past 500 years (from roughly 1480 to 1990), while tracers for anthropogenic pollution did increase markedly.

The formation of Arctic haze is related to the fact that during winter months, air masses from midlatitudes can transport aerosol particles into the Arctic (Heidam et al., 1999; Stohl, 2006). In contrast, in the summer months the Arctic lower atmosphere is effectively isolated and the transport of atmospheric aerosol particles into the Arctic is low (Heidam et al., 1999; Stohl, 2006). Hence, the increase in N_{INP} observed here in late spring and summer has to originate from Arctic sources, including local ones situated close to the measurement site.

Once Arctic haze is removed by precipitation in spring (Browse et al., 2012), Arctic particles are mostly newly formed particles in the size range up to 100 nm (Lange et al., 2018), originating from gaseous precursors (Engvall et al., 2008; Leaitch et al., 2013; Croft et al., 2016; Wentworth

et al., 2016; Dall'Osto et al., 2018). New particle formation ceases in late summer or early fall, and until Arctic haze sets in again later in winter, the total particle number concentration is at its lowest at well below 100 cm^{-3} . But newly formed particles do not contribute to INPs unless subject to particular conditions at cirrus level (Kanji et al., 2017). Nor does their annual cycle follow what we observed for N_{INP} , as concentrations for newly formed particles decrease much earlier in the year than observed for N_{INP} .

Arctic concentrations of mineral dust particles have been measured and modeled (Fan, 2013; Zwaafink et al., 2016) and were described to largely depend on long-range transport, with largest concentrations occurring in spring. However, dust from local sources may also contribute (Zwaafink et al., 2016). Mineral dust particles themselves likely only become ice active at T at the lower end of or below those examined in the present study, but they may be carriers of biogenic ice-active macromolecules (Conen et al., 2011; Tobo et al., 2014; O'Sullivan et al., 2014; Augustin-Bauditz et al., 2016; O'Sullivan et al., 2016; Hill et al., 2016). Continental sources of fungal spores were found to contribute to the organic aerosol observed in the Arctic in summer (Fu et al., 2013), and it is known that spores of some fungal species are ice active at comparably high T (Pummer et al., 2015). The same also holds for lichen (Moffett et al., 2015) and bacteria (Hartmann et al., 2013). Sources and abundance of bacteria were examined for an area in southwest Greenland (Santl-Temkiv et al., 2018), and roughly half of all airborne bacterial cells were described to originate from local terrestrial environments such as surface soils, while the other half was said to have been long-range transported, originating from marine, glaciated, and terrestrial surfaces. In summary, microorganisms originating from continental sources in general could contribute to the highly ice-active INPs observed in this study. This is in line with the observation presented in Fig. 6, in which, particularly for VRS and Ny-Ålesund, highly ice-active INPs were observed for air masses that traveled over open land.

Particle generation at open leads in the Arctic has been observed (Held et al., 2011) in relation to sea spray from bubble production mechanisms that exist independently of wind (Norris et al., 2011). Leck and Bigg (2005) found particles in Arctic aerosol that could be attributed to algal exopolymer secretions and suggest they became airborne via bubble bursting. This agrees with observations by Orellana et al. (2011) and Fu et al. (2015), showing that Arctic marine microgels from algae, present both in surface water and SML, contribute to Arctic atmospheric particles. Such microgels were assumed to be related to INPs observed in marine SML (Wilson et al., 2015). It was recently found that ice activity in Arctic seawater was negatively correlated with salinity (Irish et al., 2017), possibly indicating that these aquatic INPs were associated with melting sea ice releasing ice-active biogenic material into the ocean. Marginal ice zones are known to be of importance for phytoplankton blooms due to melt-

ing sea ice releasing iron (Wang et al., 2014). Overall, although the abovementioned particle production mechanism in Arctic open leads was found to be only of minor importance for the overall atmospheric particle number concentration (Held et al., 2011), this, together with wind-driven sea spray production, could be a source for at least some of the highly ice-active INPs observed in our measurements. This likely holds for Alert, but it may also be the case in the example of Utqiagvik, for which in April and May very few contributions from open land or open sea, as defined by the IMS maps, were found, while highly ice-active INPs were present. These could potentially originate from open leads or polynyas. It should be added that Creamean et al. (2018a) found a similarly large increase in highly ice-active INPs during May at Oliktok Point in northern Alaska, only roughly 300 km east of Utqiagvik. This increase was related to INPs from tundra surfaces and open water, particularly the marginal ice zone. Polynyas 700 km away from the measurement site were not found to contribute, likely due to settling of particles during the long traveling times in the slow-moving air masses that were observed.

In summary, while anthropogenic pollution and new particle formation do not explain the highly ice-active INPs observed in this study, these INPs can originate from both terrestrial and marine sources in the Arctic. These sources are strong in summer and weak or absent in winter, depending on the conditions on the ground. Should terrestrial sources be found to contribute more strongly than marine ones, N_{INP} values further away from land will be lower than those observed here.

Concerning Arctic mixed-phase clouds at temperatures above -20°C , recently Norgren et al. (2018) observed a depression of cloud ice in these clouds when they are polluted, as observed during Arctic haze. Under these conditions, they have a lower amount of cloud ice mass for a given amount of condensed liquid mass. Based on the results presented here, this can be explained by the lower concentrations of INPs during times of Arctic haze – a reasoning that sheds light on the importance of the findings reported here, which could not yet have been discussed in Norgren et al. (2018). With respect to recent modeling results, Solomon et al. (2018) did large-eddy simulation (LES) studies of Arctic mixed-phase stratocumulus clouds and found indications that changes in INPs in Arctic aerosol dominate over changes in cloud condensation nuclei (CCN). This shows the potential importance of determining INPs and their changes due to climate change in the Arctic. However, Taylor et al. (2018) examined the Arctic annual cycle in cloud amounts from 24 different models and found significant disagreements. They conclude that the parameterization of ice microphysics in the models contributes to the observed differences. Overall, the field of Arctic mixed-phase clouds and related ice nucleation is currently one of intense research, and the results presented herein contribute to our understanding and lay a foundation for improved descriptions of INPs in modeling in the future.

6 Summary and conclusions

This study shows a yearly cycle of N_{INP} at four different Arctic sites, an observation that has not been seen so clearly in previous studies. Maximum values were observed roughly from late spring until well into fall, and minimum values were observed during winter and early spring. INP spectra for the most ice-active INPs are close to some observed at continental locations outside of the Arctic (Petters and Wright, 2015). Potential source regions for INPs that are ice active at the higher examined T were determined based on combining air mass back trajectories with IMS satellite maps. Such source regions were found in the Arctic on open land as well as on open water, particularly in Baffin Bay, along the southern part of the west coast of Greenland, and on Svalbard and the adjacent sea. Contributions from these regions could explain the increase in highly ice-active INPs observed in spring in Alert, Ny-Ålesund, and VRS. However, a possible source region for the highly ice-active INPs observed in Utqiagvik could not be identified. Here, highly ice-active INPs appeared earlier in the year than at the other stations. Open leads and polynyas present in the Arctic sea ice are not identified as open water in IMS maps and may have contributed to these INPs.

Regions that were not identified as source regions for highly ice-active INPs in this study may still contribute such INPs. It should be mentioned that source regions determined here were mostly on or close to land. We showed that there is a large scatter in the literature values observed for N_{INP} in the Arctic. As we find a yearly cycle in Arctic N_{INP} , this large scatter may partially originate from the different times of the year when samples were taken. It may also depend on the proximity to land where the sampling was done if terrestrial sources and sources in close proximity to land are shown to be dominant for highly ice-active INPs in the future.

Independent of their origin, these observed INPs might be transported certain distances and might have more than only local influences. This can become important, as biogenic emissions in general can be expected to increase in the Arctic in coming years due to Arctic amplification, which amplifies marine primary production (Arrigo et al., 2008; Ardyna et al., 2014) and changes Arctic microbial communities (Deslippe et al., 2012). Feedback mechanisms involving ice formation, along with radiative properties and lifetimes of Arctic stratiform clouds, may exist and be related to biogenic INPs. Therefore, more thorough studies concerning Arctic INPs are needed. Determining the current status of INPs in the Arctic and future changes that are to be expected might help us to understand aerosol–cloud interactions in the Arctic and their significance for the observed strong Arctic warming.

Data availability. Data (frozen fractions and INP concentrations) are available on Pangaea (<https://doi.pangaea.de/10.1594/PANGAEA.899701>; Wex et al., 2019).

Supplement. The supplement related to this article is available online at: <https://doi.org/10.5194/acp-19-5293-2019-supplement>.

Author contributions. HW and FS designed the research; RJS, TEB, RT, SB, RB, HS, LH, WZ, and HH did field campaign management and/or filter sampling; TEB, CEM, and WZ did chemical analysis; MH calibrated and JL, ML, and OL operated the ice nucleation measurement device; PH calculated trajectories; AH did the work on the satellite data; HW analyzed the data and wrote the paper with contributions from LH, HH, RJS, CEM, RT, FS, MH, PH, ML, RB, HS, and WZ.

Competing interests. The authors declare that they have no conflict of interest.

Special issue statement. This article is part of the special issue “Arctic mixed-phase clouds as studied during the ACLOUD/PASCAL campaigns in the framework of (AC)³ (ACP/AMT inter-journal SI)”. It is not associated with a conference.

Acknowledgements. We gratefully acknowledge the funding from the Deutsche Forschungsgemeinschaft (DFG, German Research Foundation; project number 268020496, TRR 172) within the Transregional Collaborative Research Center “Arctic Amplification: Climate Relevant Atmospheric and Surface Processes, and Feedback Mechanisms (AC)³” for filter analysis and interpretations done in subproject B04. Heike Wex was partially funded by DFG within the Ice Nuclei research Unit (INUIT, FOR 1525), WE 4722/1-2. We acknowledge Cecilia Shin, Darrell Ernst, and Andrew Platt for logistic support, fieldwork in Alert, and assistance in analysis, as well as the Canadian Forces Station Alert for supporting sample collection. Logistic assistance of the Polar Support Unit of the CNR (Italian National Research Council) Department of Earth and Environment (POLARNET) in coordinating the activities based at the Dirigibile Italia Arctic station at Ny-Ålesund is acknowledged, specifically Mauro Mazzola and Angelo Viola. Financial and technical support for samples from Utqiagvik was provided by the United States Department of Energy (Atmospheric Radiation Measurement field campaign no. 2010-05876), NOAA (award no. NA14OAR4310150), and the C. Gus Glasscock, Jr. Endowed Fund for Excellence in Environmental Sciences. We also thank Walter Brower and Jimmy Ivanoff of the Ukpeaġvik Iñupiat Corporation for sample collection and field assistance and Fred Helsel, Dan Lucero, Jeffrey Zirzow, and the Sandia National Laboratory for site access and preparation. The work at Villum Research Station at Station Nord was financially supported by the Danish Environmental Protection Agency and Energy Agency via the MIKA/DANCEA funds for Environmental Support to the Arctic Region, which is part of the Danish contribution to

the Arctic Monitoring and Assessment Programme (AMAP) and to the Danish research project “Short-Lived Climate Forcers” (SLCF). The Villum Foundation is acknowledged for funding the construction of Villum Research Station, Station Nord. The authors gratefully acknowledge the NOAA Air Resources Laboratory (ARL) for the provision of the HYSPLIT transport and dispersion model and/or READY website (<http://www.ready.noaa.gov>, last access: 13 April 2019) used in this publication. And furthermore, we thank Richard Leitch (ECCC) for helpful discussions during the writing process.

The publication of this article was funded by the Open Access Fund of the Leibniz Association.

Review statement. This paper was edited by Amy Solomon and reviewed by Paul DeMott and one anonymous referee.

References

- Ansmann, A., Tesche, M., Seifert, P., Althausen, D., Engelmann, R., Fruntke, J., Wandinger, U., Mattis, I., and Müller, D.: Evolution of the ice phase in tropical altocumulus: SAMUM lidar observations over Cape Verde, *J. Geophys. Res.*, 114, D17208, <https://doi.org/10.1029/2008JD011659>, 2009.
- Ardyna, M., Babin, M., Gosselin, M., Devred, E., Rainville, L., and Tremblay, J.-E.: Recent Arctic Ocean sea ice loss triggers novel fall phytoplankton blooms, *Geophys. Res. Lett.*, 41, 6207–6212, <https://doi.org/10.1002/2014gl061047>, 2014.
- Arrigo, K. R., van Dijken, G., and Pabi, S.: Impact of a shrinking Arctic ice cover on marine primary production, *Geophys. Res. Lett.*, 35, L19603, <https://doi.org/10.1029/2008gl035028>, 2008.
- Augustin-Bauditz, S., Wex, H., Kanter, S., Ebert, M., Stolz, F., Prager, A., Niedermeier, D., and Stratmann, F.: The immersion mode ice nucleation behavior of mineral dusts: A comparison of different pure and surface modified dusts, *Geophys. Res. Lett.*, 41, 7375–7382, <https://doi.org/10.1002/2014GL061317>, 2014.
- Augustin-Bauditz, S., Wex, H., Denjean, C., Hartmann, S., Schneider, J., Schmidt, S., Ebert, M., and Stratmann, F.: Laboratory-generated mixtures of mineral dust particles with biological substances: characterization of the particle mixing state and immersion freezing behavior, *Atmos. Chem. Phys.*, 16, 5531–5543, <https://doi.org/10.5194/acp-16-5531-2016>, 2016.
- Barrett, T. E. and Sheesley, R. J.: Year-round optical properties and source characterization of Arctic organic carbon aerosols on the North Slope Alaska, *J. Geophys. Res.*, 122, 9319–9331, <https://doi.org/10.1002/2016JD026194>, 2017.
- Bigg, E. K.: Ice forming nuclei in the high Arctic, *Tellus B*, 48, 223–233, <https://doi.org/10.1034/j.1600-0889.1996.t01-1-00007.x>, 1996.
- Bigg, E. K. and Leck, C.: Cloud-active particles over the central Arctic Ocean, *J. Geophys. Res.-Atmos.*, 106, 32155–32166, <https://doi.org/10.1029/1999jd901152>, 2001.
- Borys, R. D.: The effects of long-range transport of air pollutants on Arctic cloud-active aerosol, Thesis, Atmospheric Science Paper No. 367, Colorado State University, Fort Collins, Colorado, USA, 1983.
- Borys, R. D.: Studies of ice nucleation by Arctic aerosol on AGASP-II, *J. Atmos. Chem.*, 9, 169–185, <https://doi.org/10.1007/bf00052831>, 1989.
- Bossi, R., Vorkamp, K., and Skov, H.: Concentrations of organochlorine pesticides, polybrominated diphenyl ethers and perfluorinated compounds in the atmosphere of North Greenland, *Environ. Pollut.*, 217, 4–10, <https://doi.org/10.1016/j.envpol.2015.12.026>, 2016.
- Browse, J., Carslaw, K. S., Arnold, S. R., Pringle, K., and Boucher, O.: The scavenging processes controlling the seasonal cycle in Arctic sulphate and black carbon aerosol, *Atmos. Chem. Phys.*, 12, 6775–6798, <https://doi.org/10.5194/acp-12-6775-2012>, 2012.
- Burrows, S. M., Hoose, C., Pöschl, U., and Lawrence, M. G.: Ice nuclei in marine air: biogenic particles or dust?, *Atmos. Chem. Phys.*, 13, 245–267, <https://doi.org/10.5194/acp-13-245-2013>, 2013.
- Chan, T. W., Huang, L., Leitch, W. R., Sharma, S., Brook, J. R., Slowik, J. G., Abbatt, J. P. D., Brickell, P. C., Liggio, J., Li, S.-M., and Moosmüller, H.: Observations of OM / OC and specific attenuation coefficients (SAC) in ambient fine PM at a rural site in central Ontario, Canada, *Atmos. Chem. Phys.*, 10, 2393–2411, <https://doi.org/10.5194/acp-10-2393-2010>, 2010.
- Chen, J., Wu, Z., Augustin-Bauditz, S., Grawe, S., Hartmann, M., Pei, X., Liu, Z., Ji, D., and Wex, H.: Ice-nucleating particle concentrations unaffected by urban air pollution in Beijing, China, *Atmos. Chem. Phys.*, 18, 3523–3539, <https://doi.org/10.5194/acp-18-3523-2018>, 2018.
- Choi, Y. S., Lindzen, R. S., Ho, C. H., and Kim, J.: Space observations of cold-cloud phase change, *P. Natl. Acad. Sci. USA*, 107, 11211–11216, <https://doi.org/10.1073/pnas.1006241107>, 2010.
- Cohen, J., Screen, J. A., Furtado, J. C., Barlow, M., Whittleston, D., Coumou, D., Francis, J., Dethloff, K., Entekhabi, D., Overland, J., and Jones, J.: Recent Arctic amplification and extreme mid-latitude weather, *Nat. Geosci.*, 7, 627–637, <https://doi.org/10.1038/ngeo2234>, 2014.
- Conen, F., Morris, C. E., Leifeld, J., Yakutin, M. V., and Alewell, C.: Biological residues define the ice nucleation properties of soil dust, *Atmos. Chem. Phys.*, 11, 9643–9648, <https://doi.org/10.5194/acp-11-9643-2011>, 2011.
- Conen, F., Henne, S., Morris, C. E., and Alewell, C.: Atmospheric ice nucleators active = -12°C can be quantified on PM₁₀ filters, *Atmos. Meas. Tech.*, 5, 321–327, <https://doi.org/10.5194/amt-5-321-2012>, 2012.
- Conen, F., Stopelli, E., and Zimmermann, L.: Clues that decaying leaves enrich Arctic air with ice nucleating particles, *Atmos. Environ.*, 129, 91–94, <https://doi.org/10.1016/j.atmosenv.2016.01.027>, 2016.
- Costa, A., Meyer, J., Afchine, A., Luebke, A., Günther, G., Dorsey, J. R., Gallagher, M. W., Ehrlich, A., Wendisch, M., Baumgardner, D., Wex, H., and Krämer, M.: Classification of Arctic, midlatitude and tropical clouds in the mixed-phase temperature regime, *Atmos. Chem. Phys.*, 17, 12219–12238, <https://doi.org/10.5194/acp-17-12219-2017>, 2017.
- Creamean, J. M., Kirpes, R. M., Pratt, K. A., Spada, N. J., Maahn, M., de Boer, G., Schnell, R. C., and China, S.: Marine and terrestrial influences on ice nucleating particles during continuous springtime measurements in an Arctic oilfield location, *Atmos.*

- Chem. Phys., 18, 18023–18042, <https://doi.org/10.5194/acp-18-18023-2018>, 2018a.
- Creamean, J. M., Mignani, C., Bukowiecki, N., and Conen, F.: Using spectra characteristics to identify ice nucleating particle populations during winter storms in the Alps, *Atmos. Chem. Phys. Discuss.*, <https://doi.org/10.5194/acp-2018-1082>, in review, 2018b.
- Croft, B., Wentworth, G. R., Martin, R. V., Leaitch, W. R., Murphy, J. G., Murphy, B. N., Kodros, J. K., Abbatt, J. P. D., and Pierce, J. R.: Contribution of Arctic seabird-colony ammonia to atmospheric particles and cloud-albedo radiative effect, *Nat. Commun.*, 7, 13444, <https://doi.org/10.1038/ncomms13444>, 2016.
- Dall'Osto, M., Simo, R., Harrison, R. M., Beddows, D. C. S., Saiz-Lopez, A., Lange, R., Skov, H., Nojgaard, J. K., Nielsen, I. E., and Massling, A.: Abiotic and biotic sources influencing spring new particle formation in North East Greenland, *Atmos. Environ.*, 190, 126–134, <https://doi.org/10.1016/j.atmosenv.2018.07.019>, 2018.
- de Boer, G., Morrison, H., Shupe, M. D., and Hildner, R.: Evidence of liquid dependent ice nucleation in high-latitude stratiform clouds from surface remote sensors, *Geophys. Res. Lett.*, 38, L01803, <https://doi.org/10.1029/2010gl046016>, 2011.
- DeMott, P. J., Hill, T. C. J., McCluskey, C. S., Prather, K. A., Collins, D. B., Sullivan, R. C., Ruppel, M. J., Mason, R. H., Irish, V. E., Lee, T., Hwang, C. Y., Rhee, T. S., Snider, J. R., McMeeking, G. R., Dhaniyala, S., Lewis, E. R., Wentzell, J. J. B., Abbatt, J., Lee, C., Sultana, C. M., Ault, A. P., Axson, J. L., Diaz Martinez, M., Venero, I., Santos-Figueroa, G., Stokes, M. D., Deane, G. B., Mayol-Bracero, O. L., Grassian, V. H., Bertram, T. H., Bertram, A. K., Moffett, B. F., and Franc, G. D.: Sea spray aerosol as a unique source of ice nucleating particles, *P. Natl. Acad. Sci. USA*, 113, 5797–5803, <https://doi.org/10.1073/pnas.1514034112>, 2016.
- Deslippe, J. R., Hartmann, M., Simard, S. W., and Mohn, W. W.: Long-term warming alters the composition of Arctic soil microbial communities, 82, 303–315, <https://doi.org/10.1111/j.1574-6941.2012.01350.x>, 2012.
- Engvall, A.-C., Krejci, R., Ström, J., Treffeisen, R., Scheele, R., Hermansen, O., and Paatero, J.: Changes in aerosol properties during spring-summer period in the Arctic troposphere, *Atmos. Chem. Phys.*, 8, 445–462, <https://doi.org/10.5194/acp-8-445-2008>, 2008.
- Fan, S. M.: Modeling of observed mineral dust aerosols in the arctic and the impact on winter season low-level clouds, *J. Geophys. Res.-Atmos.*, 118, 11161–11174, <https://doi.org/10.1002/jgrd.50842>, 2013.
- Freud, E., Krejci, R., Tunved, P., Leaitch, R., Nguyen, Q. T., Massling, A., Skov, H., and Barrie, L.: Pan-Arctic aerosol number size distributions: seasonality and transport patterns, *Atmos. Chem. Phys.*, 17, 8101–8128, <https://doi.org/10.5194/acp-17-8101-2017>, 2017.
- Fu, P. Q., Kawamura, K., Chen, J., Charrière, B., and Sempéré, R.: Organic molecular composition of marine aerosols over the Arctic Ocean in summer: contributions of primary emission and secondary aerosol formation, *Biogeosciences*, 10, 653–667, <https://doi.org/10.5194/bg-10-653-2013>, 2013.
- Fu, P. Q., Kawamura, K., Chen, J., Qin, M. Y., Ren, L. J., Sun, Y. L., Wang, Z. F., Barrie, L. A., Tachibana, E., Ding, A. J., and Yamashita, Y.: Fluorescent water-soluble organic aerosols in the High Arctic atmosphere, *Sci. Rep.*, 5, 9845, <https://doi.org/10.1038/srep09845>, 2015.
- Harrison, A. D., Whale, T. F., Carpenter, M. A., Holden, M. A., Neve, L., O'Sullivan, D., Vergara Temprado, J., and Murray, B. J.: Not all feldspars are equal: a survey of ice nucleating properties across the feldspar group of minerals, *Atmos. Chem. Phys.*, 16, 10927–10940, <https://doi.org/10.5194/acp-16-10927-2016>, 2016.
- Hartmann, M., Blunier, T., Brügger, S. O., Schmale, J., Schwikowski, M., Vogel, A., Wex, H., and Stratmann, F.: Variation of ice nucleating particles in the European Arctic over the last centuries, *Geophys. Res. Lett.*, 46, <https://doi.org/10.1029/2019GL082311>, 2019.
- Hartmann, S., Augustin, S., Clauss, T., Wex, H., Šantl-Temkiv, T., Voigtländer, J., Niedermeier, D., and Stratmann, F.: Immersion freezing of ice nucleation active protein complexes, *Atmos. Chem. Phys.*, 13, 5751–5766, <https://doi.org/10.5194/acp-13-5751-2013>, 2013.
- Heidam, N. Z., Wahlin, P., and Christensen, J. H.: Tropospheric gases and aerosols in northeast Greenland, *J. Atmos. Sci.*, 56, 261–278, [https://doi.org/10.1175/1520-0469\(1999\)056<0261:tgaain>2.0.co;2](https://doi.org/10.1175/1520-0469(1999)056<0261:tgaain>2.0.co;2), 1999.
- Held, A., Brooks, I. M., Leck, C., and Tjernström, M.: On the potential contribution of open lead particle emissions to the central Arctic aerosol concentration, *Atmos. Chem. Phys.*, 11, 3093–3105, <https://doi.org/10.5194/acp-11-3093-2011>, 2011.
- Helfrich, S. R., McNamara, D., Ramsay, B. H., Baldwin, T., and Kasheta, T.: Enhancements to, and forthcoming developments in the Interactive Multisensor Snow and Ice Mapping System (IMS), *Hydrol. Process.*, 21, 1576–1586, <https://doi.org/10.1002/hyp.6720>, 2007.
- Herenz, P., Wex, H., Henning, S., Kristensen, T. B., Rubach, F., Roth, A., Borrmann, S., Bozem, H., Schulz, H., and Stratmann, F.: Measurements of aerosol and CCN properties in the Mackenzie River delta (Canadian Arctic) during spring–summer transition in May 2014, *Atmos. Chem. Phys.*, 18, 4477–4496, <https://doi.org/10.5194/acp-18-4477-2018>, 2018.
- Hill, T. C. J., DeMott, P. J., Tobo, Y., Fröhlich-Nowoisky, J., Moffett, B. F., Franc, G. D., and Kreidenweis, S. M.: Sources of organic ice nucleating particles in soils, *Atmos. Chem. Phys.*, 16, 7195–7211, <https://doi.org/10.5194/acp-16-7195-2016>, 2016.
- Hoose, C. and Möhler, O.: Heterogeneous ice nucleation on atmospheric aerosols: a review of results from laboratory experiments, *Atmos. Chem. Phys.*, 12, 9817–9854, <https://doi.org/10.5194/acp-12-9817-2012>, 2012.
- Huang, L., Brook, J. R., Zhang, W., Li, S. M., Graham, L., Ernst, D., Chivulescu, A., and Lu, G.: Stable isotope measurements of carbon fractions (OC/EC) in airborne particulate: A new dimension for source characterization and apportionment, *Atmos. Environ.*, 40, 2690–2705, <https://doi.org/10.1016/j.atmosenv.2005.11.062>, 2006.
- Intrieri, J. M., Fairall, C. W., Shupe, M. D., Persson, P. O. G., Andreas, E. L., Guest, P. S., and Moritz, R. E.: An annual cycle of Arctic surface cloud forcing at SHEBA, *J. Geophys. Res.*, 107, 8039, <https://doi.org/10.1029/2000jc000439>, 2002.
- IPCC: Climate Change 2013: The Physical Science Basis. Contribution of Working Group I to the Fifth Assessment Report of the Intergovernmental Panel on Climate Change, edited by: Stocker, T. F., Qin, D., Plattner, G.-K., Tignor, M., Allen, S. K.,

- Boschung, J., Nauels, A., Xia, Y., Bex, V., and Midgley, P. M.: Cambridge University Press, Cambridge, UK and New York, NY, USA, <https://doi.org/10.1017/CBO9781107415324>, 2013.
- Irish, V. E., Elizondo, P., Chen, J., Chou, C., Charette, J., Lizotte, M., Ladino, L. A., Wilson, T. W., Gosselin, M., Murray, B. J., Polishchuk, E., Abbatt, J. P. D., Miller, L. A., and Bertram, A. K.: Ice-nucleating particles in Canadian Arctic sea-surface microlayer and bulk seawater, *Atmos. Chem. Phys.*, 17, 10583–10595, <https://doi.org/10.5194/acp-17-10583-2017>, 2017.
- Irish, V. E., Hanna, S. J., Willis, M. D., China, S., Thomas, J. L., Wentzell, J. J. B., Cirisan, A., Si, M., Leaitch, W. R., Murphy, J. G., Abbatt, J. P. D., Laskin, A., Girard, E., and Bertram, A. K.: Ice nucleating particles in the marine boundary layer in the Canadian Arctic during summer 2014, *Atmos. Chem. Phys.*, 19, 1027–1039, <https://doi.org/10.5194/acp-19-1027-2019>, 2019.
- Kalesse, H., de Boer, G., Solomon, A., Oue, M., Ahlgrimm, M., Zhang, D. M., Shupe, M. D., Luke, E., and Protat, A.: Understanding Rapid Changes in Phase Partitioning between Cloud Liquid and Ice in Stratiform Mixed-Phase Clouds: An Arctic Case Study, *Mon. Weather Rev.*, 144, 4805–4826, <https://doi.org/10.1175/mwr-d-16-0155.1>, 2016.
- Kanji, Z. A., Ladino, L. A., Wex, H., Boose, Y., Kohn, M., Cziczo, D., and Krämer, M.: Overview of Ice Nucleating Particles, chap. 1, vol. 58, *Meteor. Monogr.*, <https://doi.org/10.1175/AMSMONOGRAPHS-D-16-0006.1>, 2017.
- Lange, R., Dall’Osto, M., Skov, H., Nøjgaard, J., Nielsen, I. E., Beddows, D., Simo, R., Harrison, R. M., and Massling, A.: Characterization of distinct Arctic aerosol accumulation modes and their sources, *Atmos. Environ.*, 183, 1–10, <https://doi.org/10.1016/j.atmosenv.2018.03.060>, 2018.
- Leaitch, W. R., Sharma, S., Huang, L., Toom-Saunty, D., Chivulescu, A., Macdonald, A. M., von Salzen, K., Pierce, J. R., Bertram, A. K., Schroder, J. C., Shantz, N. C., Chang, R. Y.-W., and Norman, A.-L.: Dimethyl sulfide control of the clean summertime Arctic aerosol and cloud, *Elem. Sci. Anthr.*, 1, p. 000017, <https://doi.org/10.12952/journal.elementa.000017>, 2013.
- Leck, C. and Bigg, E. K.: Biogenic particles in the surface microlayer and overlaying atmosphere in the central Arctic Ocean during summer, *Tellus B*, 57, 305–316, <https://doi.org/10.1111/j.1600-0889.2005.00148.x>, 2005.
- Loewe, K., Ekman, A. M. L., Paukert, M., Sedlar, J., Tjernström, M., and Hoose, C.: Modelling micro- and macrophysical contributors to the dissipation of an Arctic mixed-phase cloud during the Arctic Summer Cloud Ocean Study (ASCOS), *Atmos. Chem. Phys.*, 17, 6693–6704, <https://doi.org/10.5194/acp-17-6693-2017>, 2017.
- Mason, R. H., Si, M., Chou, C., Irish, V. E., Dickie, R., Elizondo, P., Wong, R., Brintnell, M., Elsasser, M., Lassar, W. M., Pierce, K. M., Leaitch, W. R., Macdonald, A. M., Platt, A., Toom-Saunty, D., Sarda-Estève, R., Schiller, C. L., Suski, K. J., Hill, T. C. J., Abbatt, J. P. D., Huffman, J. A., DeMott, P. J., and Bertram, A. K.: Size-resolved measurements of ice-nucleating particles at six locations in North America and one in Europe, *Atmos. Chem. Phys.*, 16, 1637–1651, <https://doi.org/10.5194/acp-16-1637-2016>, 2016.
- McCluskey, C. S., Hill, T. C. J., Humphries, R. S., Rauker, A. M., Moreau, S., Stratton, P. G., Chambers, S. D., Williams, A. G., McRobert, I., Ward, J., Keywood, M. D., Harnwell, J., Ponsonby, W., Loh, Z. M., Krummel, P. B., Protat, A., Kreidenweis, S. M., and DeMott, P. J.: Observations of Ice Nucleating Particles Over Southern Ocean Waters, *Geophys. Res. Lett.*, 45, 11989–11997, <https://doi.org/10.1029/2018gl079981>, 2018a.
- McCluskey, C. S., Ovadnevaite, J., Rinaldi, M., Atkinson, J., Berosi, F., Ceburnis, D., Marullo, S., Hill, T. C. J., Lohmann, U., Kanji, Z. A., O’Dowd, C., Kreidenweis, S. M., and DeMott, P. J.: Marine and Terrestrial Organic Ice-Nucleating Particles in Pristine Marine to Continentally Influenced Northeast Atlantic Air Masses, *J. Geophys. Res.-Atmos.*, 123, 6196–6212, <https://doi.org/10.1029/2017jd028033>, 2018b.
- Moffett, B. F., Getti, G., Henderson-Begg, S. K., and Hill, T. C. J.: Ubiquity of ice nucleation in lichen – possible atmospheric implications, *Lindbergia*, 38, 39–43, 2015.
- Morrison, H., de Boer, G., Feingold, G., Harrington, J., Shupe, M. D., and Sulia, K.: Resilience of persistent Arctic mixed-phase clouds, *Nat. Geosci.*, 5, 11–17, <https://doi.org/10.1038/ngeo1332>, 2012.
- Murray, B. J., O’Sullivan, D., Atkinson, J. D., and Webb, M. E.: Ice nucleation by particles immersed in supercooled cloud droplets, *Chem. Soc. Rev.*, 41, 6519–6554, 2012.
- National-Ice-Center: 2008, updated daily. IMS Daily Northern Hemisphere Snow and Ice Analysis at 1 km, 4 km, and 24 km Resolutions, Version 1, Boulder, Colorado USA. NSIDC: National Snow and Ice Data Center, accessed on 27 September 2018, <https://doi.org/10.7265/N52R3PMC>, 2008.
- Nguyen, Q. T., Glasius, M., Sørensen, L. L., Jensen, B., Skov, H., Birmili, W., Wiedensohler, A., Kristensson, A., Nøjgaard, J. K., and Massling, A.: Seasonal variation of atmospheric particle number concentrations, new particle formation and atmospheric oxidation capacity at the high Arctic site Villum Research Station, Station Nord, *Atmos. Chem. Phys.*, 16, 11319–11336, <https://doi.org/10.5194/acp-16-11319-2016>, 2016.
- Norgren, M. S., de Boer, G., and Shupe, M. D.: Observed aerosol suppression of cloud ice in low-level Arctic mixed-phase clouds, *Atmos. Chem. Phys.*, 18, 13345–13361, <https://doi.org/10.5194/acp-18-13345-2018>, 2018.
- Norris, S. J., Brooks, I. M., de Leeuw, G., Sirevaag, A., Leck, C., Brooks, B. J., Birch, C. E., and Tjernström, M.: Measurements of bubble size spectra within leads in the Arctic summer pack ice, *Ocean Sci.*, 7, 129–139, <https://doi.org/10.5194/os-7-129-2011>, 2011.
- Orellana, M. V., Matrai, P. A., Leck, C., Rauschenberg, C. D., Lee, A. M., and Coz, E.: Marine microgels as a source of cloud condensation nuclei in the high Arctic, *P. Natl. Acad. Sci. USA*, 108, 13612–13617, <https://doi.org/10.1073/pnas.1102457108>, 2011.
- O’Sullivan, D., Murray, B. J., Malkin, T. L., Whale, T. F., Umo, N. S., Atkinson, J. D., Price, H. C., Baustian, K. J., Browse, J., and Webb, M. E.: Ice nucleation by fertile soil dusts: relative importance of mineral and biogenic components, *Atmos. Chem. Phys.*, 14, 1853–1867, <https://doi.org/10.5194/acp-14-1853-2014>, 2014.
- O’Sullivan, D., Murray, B. J., Ross, J. F., and Webb, M. E.: The adsorption of fungal ice-nucleating proteins on mineral dusts: a terrestrial reservoir of atmospheric ice-nucleating particles, *Atmos. Chem. Phys.*, 16, 7879–7887, <https://doi.org/10.5194/acp-16-7879-2016>, 2016.

- O'Sullivan, D., Adams, M. P., Tarn, M. D., Harrison, A. D., Vergara-Temprado, J., Porter, G. C. E., Holden, M. A., Sanchez-Marroquin, A., Carotenuto, F., Whale, T. F., McQuaid, J. B., Walshaw, R., Hedges, D. H. P., Burke, I. T., Cui, Z., and Murray, B. J.: Contributions of biogenic material to the atmospheric ice-nucleating particle population in North Western Europe, *Sci. Rep.*, 8, 13821, <https://doi.org/10.1038/s41598-018-31981-7>, 2018.
- Ovchinnikov, M., Ackerman, A. S., Avramov, A., Cheng, A. N., Fan, J. W., Fridlind, A. M., Ghan, S., Harrington, J., Hoose, C., Korolev, A., McFarquhar, G. M., Morrison, H., Paukert, M., Savre, J., Shipway, B. J., Shupe, M. D., Solomon, A., and Sulia, K.: Intercomparison of large-eddy simulations of Arctic mixed-phase clouds: Importance of ice size distribution assumptions, *J. Adv. Model Earth Syst.*, 6, 223–248, <https://doi.org/10.1002/2013ms000282>, 2014.
- Petters, M. D. and Wright, T. P.: Revisiting ice nucleation from precipitation samples, *Geophys. Res. Lett.*, 42, 8758–8766, <https://doi.org/10.1002/2015gl065733>, 2015.
- Pithan, F. and Mauritsen, T.: Arctic amplification dominated by temperature feedbacks in contemporary climate models, *Nat. Geosci.*, 7, 181–184, <https://doi.org/10.1038/ngeo2071>, 2014.
- Polen, M., Lawlis, E., and Sullivan, R. C.: The unstable ice nucleation properties of Snomax (R) bacterial particles, *J. Geophys. Res.-Atmos.*, 121, 11666–11678, <https://doi.org/10.1002/2016jd025251>, 2016.
- Prenni, A. J., Harrington, J. Y., Tjernstrom, M., DeMott, P. J., Avramov, A., Long, C. N., Kreidenweis, S. M., Olsson, P. Q., and Verlinde, J.: Can ice-nucleating aerosols affect Arctic seasonal climate?, *B. Am. Meteorol. Soc.*, 88, 541–550, <https://doi.org/10.1175/bams-88-4-541>, 2007.
- Pummer, B. G., Budke, C., Augustin-Bauditz, S., Niedermeier, D., Felgitsch, L., Kampf, C. J., Huber, R. G., Liedl, K. R., Loerting, T., Moschen, T., Schauer, M., Tollinger, M., Morris, C. E., Wex, H., Grothe, H., Pöschl, U., Koop, T., and Fröhlich-Nowoisky, J.: Ice nucleation by water-soluble macromolecules, *Atmos. Chem. Phys.*, 15, 4077–4091, <https://doi.org/10.5194/acp-15-4077-2015>, 2015.
- Rogers, D. C., DeMott, P. J., and Kreidenweis, S. M.: Airborne measurements of tropospheric ice-nucleating aerosol particles in the Arctic spring, *J. Geophys. Res.*, 106, 15053–15063, 2001.
- Santl-Temkiv, T., Gosewinkel, U., Starnawski, P., Lever, M., and Finster, K.: Aeolian dispersal of bacteria in southwest Greenland: their sources, abundance, diversity and physiological states, *FEMS Microbiol. Ecol.*, 94, fty031, <https://doi.org/10.1093/femsec/fty031>, 2018.
- Schnell, R. C. and Vali, G.: Biogenic ice nuclei: Part I. Terrestrial and marine sources, *J. Atmos. Sci.*, 33, 1554–1564, 1976.
- Schnell, R. C.: Ice nuclei in seawater, fog water and marine air off coast of Nova-Scotia – summer 1975, *J. Atmos. Sci.*, 34, 1299–1305, [https://doi.org/10.1175/1520-0469\(1977\)034<1299:inisfw>2.0.co;2](https://doi.org/10.1175/1520-0469(1977)034<1299:inisfw>2.0.co;2), 1977.
- Serreze, M. C. and Barry, R. G.: Processes and impacts of Arctic amplification: A research synthesis, *Global Planet. Change*, 77, 85–96, <https://doi.org/10.1016/j.gloplacha.2011.03.004>, 2011.
- Shaw, G. E.: The Arctic haze phenomenon, *B. Am. Meteorol. Soc.*, 76, 2403–2413, [https://doi.org/10.1175/1520-0477\(1995\)076<2403:tahp>2.0.co;2](https://doi.org/10.1175/1520-0477(1995)076<2403:tahp>2.0.co;2), 1995.
- Shupe, M.: Clouds at Arctic Atmospheric Observatories. Part II: Thermodynamic Phase Characteristics, *J. Appl. Meteorol. Clim.*, 50, 645–661, <https://doi.org/10.1175/2010JAMC2468.1>, 2011.
- Shupe, M. D., Matrosov, S. Y., and Uttal, T.: Arctic mixed-phase cloud properties derived from surface-based sensors at SHEBA, *J. Atmos. Sci.*, 63, 697–711, <https://doi.org/10.1175/jas3659.1>, 2006.
- Shupe, M. D., Persson, P. O. G., Brooks, I. M., Tjernström, M., Sedlar, J., Mauritsen, T., Sjogren, S., and Leck, C.: Cloud and boundary layer interactions over the Arctic sea ice in late summer, *Atmos. Chem. Phys.*, 13, 9379–9399, <https://doi.org/10.5194/acp-13-9379-2013>, 2013.
- Si, M., Irish, V. E., Mason, R. H., Vergara-Temprado, J., Hanna, S. J., Ladino, L. A., Yakobi-Hancock, J. D., Schiller, C. L., Wentzell, J. J. B., Abbatt, J. P. D., Carslaw, K. S., Murray, B. J., and Bertram, A. K.: Ice-nucleating ability of aerosol particles and possible sources at three coastal marine sites, *Atmos. Chem. Phys.*, 18, 15669–15685, <https://doi.org/10.5194/acp-18-15669-2018>, 2018.
- Si, M., Evoy, E., Yun, J., Xi, Y., Hanna, S. J., Chivulescu, A., Rawlings, K., Veber, D., Platt, A., Kunkel, D., Hoor, P., Sharma, S., Leaitch, W. R., and Bertram, A. K.: Concentrations, composition, and sources of ice-nucleating particles in the Canadian High Arctic during spring 2016, *Atmos. Chem. Phys.*, 19, 3007–3024, <https://doi.org/10.5194/acp-19-3007-2019>, 2019.
- Solomon, A., Feingold, G., and Shupe, M. D.: The role of ice nuclei recycling in the maintenance of cloud ice in Arctic mixed-phase stratocumulus, *Atmos. Chem. Phys.*, 15, 10631–10643, <https://doi.org/10.5194/acp-15-10631-2015>, 2015.
- Solomon, A., de Boer, G., Creamean, J. M., McComiskey, A., Shupe, M. D., Maahn, M., and Cox, C.: The relative impact of cloud condensation nuclei and ice nucleating particle concentrations on phase partitioning in Arctic mixed-phase stratocumulus clouds, *Atmos. Chem. Phys.*, 18, 17047–17059, <https://doi.org/10.5194/acp-18-17047-2018>, 2018.
- Stein, A. F., Draxler, R. R., Rolph, G. D., Stunder, B. J. B., Cohen, M. D., and Ngan, F.: NOAA's HYSPLIT atmospheric transport and dispersion modeling system, *B. Am. Meteorol. Soc.*, 96, 2059–2077, <https://doi.org/10.1175/bams-d-14-00110.1>, 2015.
- Stohl, A.: Characteristics of atmospheric transport into the Arctic troposphere, *J. Geophys. Res. Atmos.*, 111, D11306, <https://doi.org/10.1029/2005jd006888>, 2006.
- Szyrmer, W. and Zawadzki, I.: Biogenic and anthropogenic sources of ice-forming nuclei: A review, *B. Am. Meteorol. Soc.*, 78, 209–228, 1997.
- Taylor, P. C., Boeke, R. C., Li, Y., and Thompson, D. W. J.: Arctic cloud annual cycle biases in climate models, *Atmos. Chem. Phys. Discuss.*, <https://doi.org/10.5194/acp-2018-1159>, in review, 2018.
- Tobo, Y., DeMott, P. J., Hill, T. C. J., Prenni, A. J., Swoboda-Colberg, N. G., Franc, G. D., and Kreidenweis, S. M.: Organic matter matters for ice nuclei of agricultural soil origin, *Atmos. Chem. Phys.*, 14, 8521–8531, <https://doi.org/10.5194/acp-14-8521-2014>, 2014.
- Tobo, Y., Adachi, K., DeMott, P. J., Hill, T. C. J., Hamilton, D. S., Mahowald, N. M., Nagatsuka, N., Ohata, S., Uetake, J., Kondo, Y., and Koike, M.: Glacially sourced dust as a potentially significant source of ice nucleating particles, *Nat. Geosci.*, 12, 253–258, <https://doi.org/10.1038/s41561-019-0314-x>, 2019.

- Tunved, P., Ström, J., and Krejci, R.: Arctic aerosol life cycle: linking aerosol size distributions observed between 2000 and 2010 with air mass transport and precipitation at Zeppelin station, Ny-Ålesund, Svalbard, *Atmos. Chem. Phys.*, 13, 3643–3660, <https://doi.org/10.5194/acp-13-3643-2013>, 2013.
- Vali, G.: Quantitative evaluation of experimental results on heterogeneous freezing nucleation of supercooled liquids, *J. Atmos. Sci.*, 28, 402–409, [https://doi.org/10.1175/1520-0469\(1971\)028<0402:qoera>2.0.co;2](https://doi.org/10.1175/1520-0469(1971)028<0402:qoera>2.0.co;2), 1971.
- Wang, S., Bailey, D., Lindsay, K., Moore, J. K., and Holland, M.: Impact of sea ice on the marine iron cycle and phytoplankton productivity, *Biogeosciences*, 11, 4713–4731, <https://doi.org/10.5194/bg-11-4713-2014>, 2014.
- Welti, A., Müller, K., Fleming, Z. L., and Stratmann, F.: Concentration and variability of ice nuclei in the subtropical maritime boundary layer, *Atmos. Chem. Phys.*, 18, 5307–5320, <https://doi.org/10.5194/acp-18-5307-2018>, 2018.
- Wentworth, G. R., Murphy, J. G., Croft, B., Martin, R. V., Pierce, J. R., Côté, J.-S., Courchesne, I., Tremblay, J.-É., Gagnon, J., Thomas, J. L., Sharma, S., Toom-Saunty, D., Chivulescu, A., Levasseur, M., and Abbatt, J. P. D.: Ammonia in the summertime Arctic marine boundary layer: sources, sinks, and implications, *Atmos. Chem. Phys.*, 16, 1937–1953, <https://doi.org/10.5194/acp-16-1937-2016>, 2016.
- Wex, H., Augustin-Bauditz, S., Boose, Y., Budke, C., Curtius, J., Diehl, K., Dreyer, A., Frank, F., Hartmann, S., Hiranuma, N., Jantsch, E., Kanji, Z. A., Kiselev, A., Koop, T., Möhler, O., Niedermeier, D., Nillius, B., Rösch, M., Rose, D., Schmidt, C., Steinke, I., and Stratmann, F.: Intercomparing different devices for the investigation of ice nucleating particles using Snomax[®] as test substance, *Atmos. Chem. Phys.*, 15, 1463–1485, <https://doi.org/10.5194/acp-15-1463-2015>, 2015.
- Wex, H., Huang, L., Sheesley, R., Bossi, R., and Traversi, R.: Annual concentrations of ice nucleating particles at different Arctic stations, PANGAEA, <https://doi.org/10.1594/PANGAEA.899701>, 2019.
- Wiacek, A., Peter, T., and Lohmann, U.: The potential influence of Asian and African mineral dust on ice, mixed-phase and liquid water clouds, *Atmos. Chem. Phys.*, 10, 8649–8667, <https://doi.org/10.5194/acp-10-8649-2010>, 2010.
- Wilson, T. W., Ladino, L. A., Alpert, P. A., Breckels, M. N., Brooks, I. M., Browse, J., Burrows, S. M., Carslaw, K. S., Huffman, J. A., Judd, C., Kilhau, W. P., Mason, R. H., McFiggans, G., Miller, L. A., Najera, J. J., Polishchuk, E., Rae, S., Schiller, C. L., Si, M., Temprado, J. V., Whale, T. F., Wong, J. P. S., Wurl, O., Yakobi-Hancock, J. D., Abbatt, J. P. D., Aller, J. Y., Bertram, A. K., Knopf, D. A., and Murray, B. J.: A marine biogenic source of atmospheric ice-nucleating particles, *Nature*, 525, 234–238, <https://doi.org/10.1038/nature14986>, 2015.
- Zwaafink, C. D. G., Grythe, H., Skov, H., and Stohl, A.: Substantial contribution of northern high-latitude sources to mineral dust in the Arctic, *J. Geophys. Res.-Atmos.*, 121, 13678–13697, <https://doi.org/10.1002/2016jd025482>, 2016.